Flux Tubes and Confinement in Lattice Quantum Chromodynamics

Leonardo Cosmai

"Bridging analytical and numerical methods for quantum field theory", FBK - ECT, Trento, 26 August 2025*

My collaborators

Marshall Baker *(Univ. of Washington, Seattle)*

Paolo Cea *(INFN, Bari)*

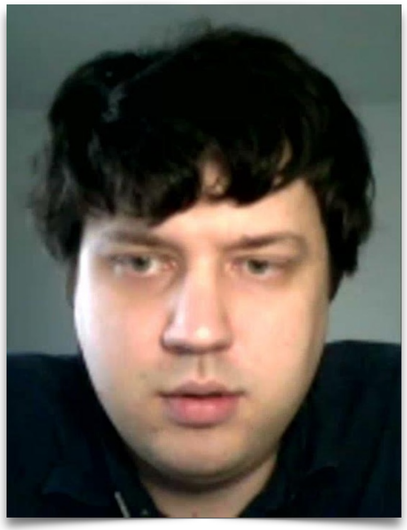

Volodymyr Chelnokov *(Goethe Universität, Frankfurt)*

Alessandro Papa *(Univ. Calabria and INFN, Cosenza)*

Numerical simulations have mainly been performed on the LEONARDO supercomputer @CINECA

LEONARDO supercomputer
250 PFlop/s - ITALY

Thanks to:

- **Cineca - INFN agreement**
- **ICSC (Italian Center for Scientific Computing)**

- LEONARDO-booster 3456 nodes
  1 x CPU Intel Xeon 8358 32 cores, 2,6 GHz
  512 (8 x 64) GB RAM DDR4 3200 MHz
  4 X Nvidia custom Ampere GPU 64GB HBM2
  2 x NVidia HDR 2×100 Gb/s cards

- LEONARDO-GP 1536 nodes
  2x Intel Sapphire Rapids, 56 cores, 4.8 GHz
  512 (16 x 32) GB RAM DDR5 4800 MHz
  3xNvidia HDR cards 1x100Gb/s cards
  8 TB NVM

THE COLOR CONFINEMENT

- Color confinement is supported by a wide range of experimental observations: in high-energy particle collisions, quarks and gluons are never observed as free particles but always emerge as part of bound states (hadrons).

- Understanding color confinement is crucial for explaining why quarks and gluons are never observed as free particles but are always confined within hadrons.

- While confinement is well supported by lattice QCD and experimental evidence, providing an analytic proof from first principles remains an open challenge in theoretical physics.

Color confinement is still an unsolved problem

https://www.claymath.org/millennium-problems/

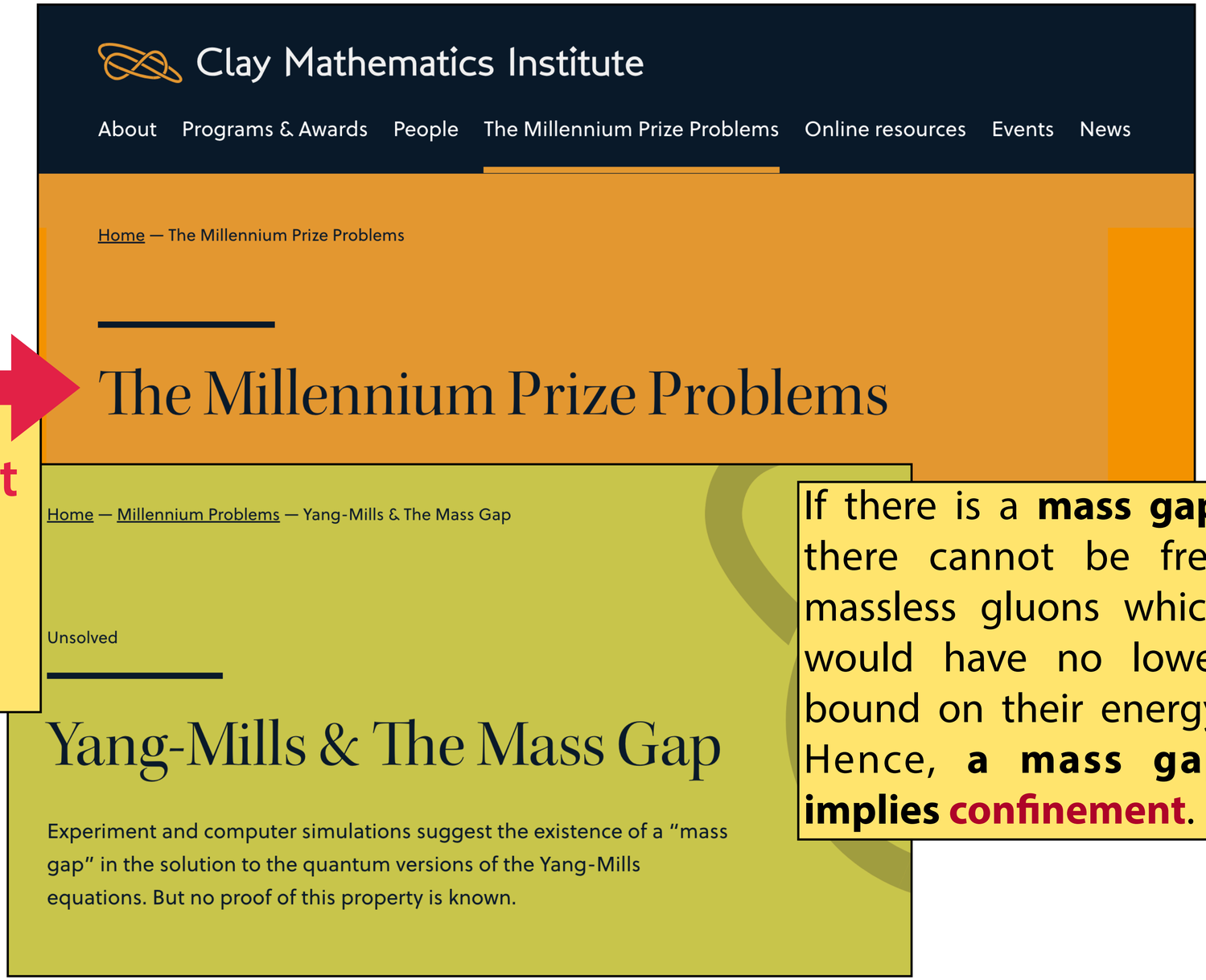

If there is a **mass gap**, there cannot be free massless gluons which would have no lower bound on their energy. Hence, **a mass gap implies confinement**.

THE COLOR CONFINEMENT (cont'd)

Heavy-quark potential – free energy of a static quark-antiquark configuration separated by a distance d.

at $T = 0$ σ**: string tension**

$$\langle W(d,t)\rangle = \exp(-t\,V(d,t))\,, \qquad \lim_{d\to\infty} V(d,t) = -\frac{c}{d} + \sigma d$$

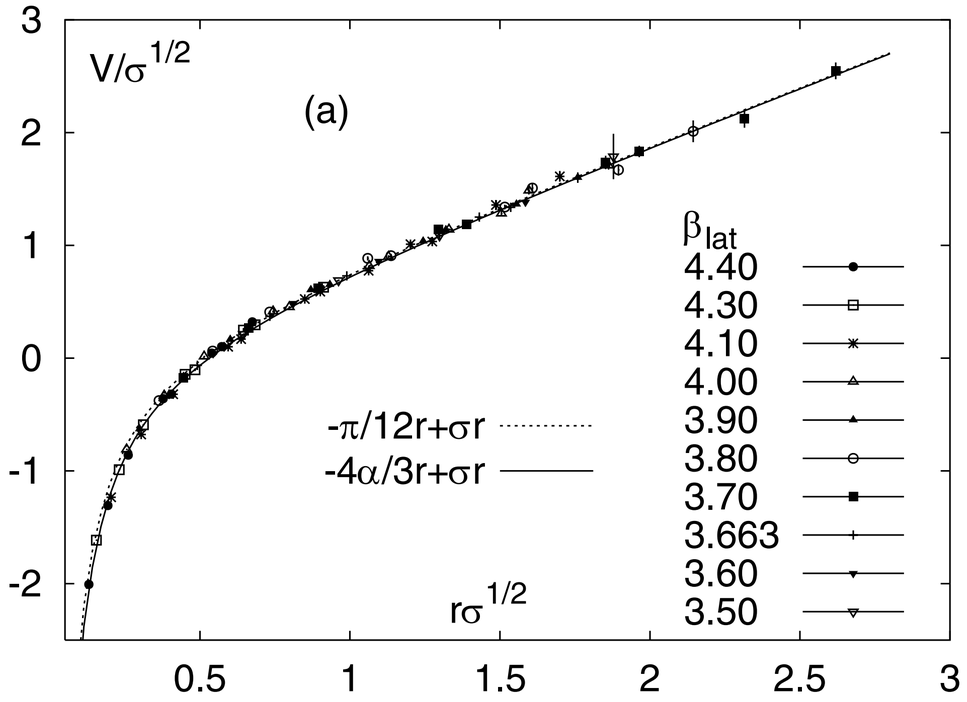

O. Kaczmarek and F. Zantow, [arXiv:hep-lat/0503017].

- Achieving a detailed understanding of color confinement remains a central goal for nonperturbative studies of QCD and is strictly related to the phase diagram of QCD.

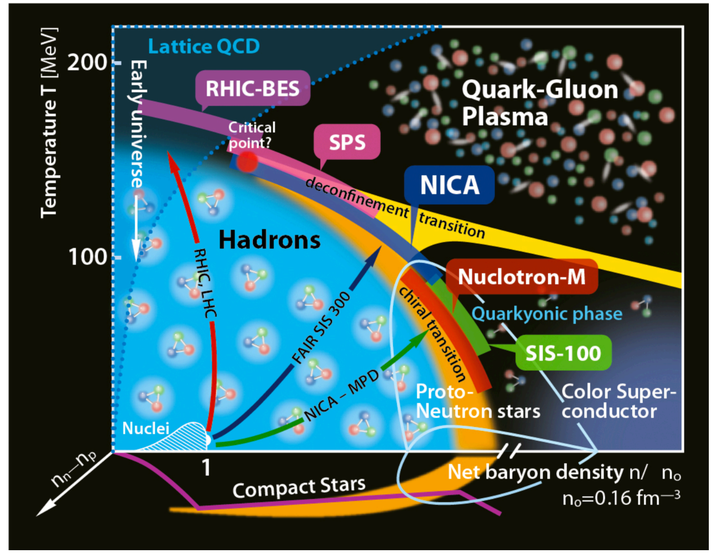

- Lattice numerical simulations have long revealed the emergence of tube-like structures when analyzing the chromoelectric fields between static quarks.

- The observation of these tube-like structures in lattice simulations is related to the linear potential between static color charges and provides direct numerical evidence for color confinement.

How to measure the chromoelectromagnetic field tensor generated by a static quark-antiquark pair separated by a distance d on the lattice?

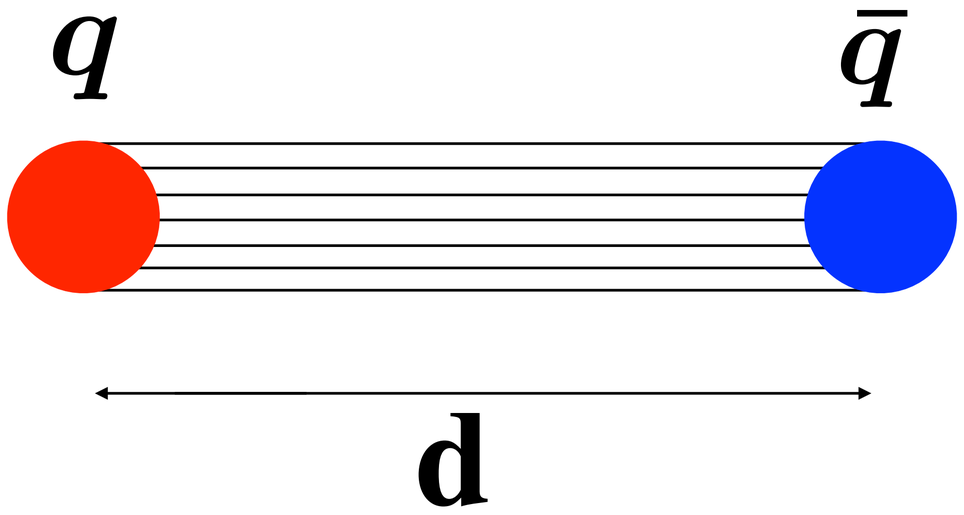

To explore on the lattice the field configurations produced by a static quark-antiquark pair —> connected correlation function (*)

(*) Di Giacomo, Maggiore, Oleínik , NPB347(1990)441

Skala, Faber, Zach, NPB494(1997)293

Kuzmenko, Simonov, PLB494(2000)81

Di Giacomo, Dosch, Shevchenko, Simonov, Phys.Rept.372(2002)319

THE SPATIAL DISTRIBUTION OF THE COLOR FIELDS

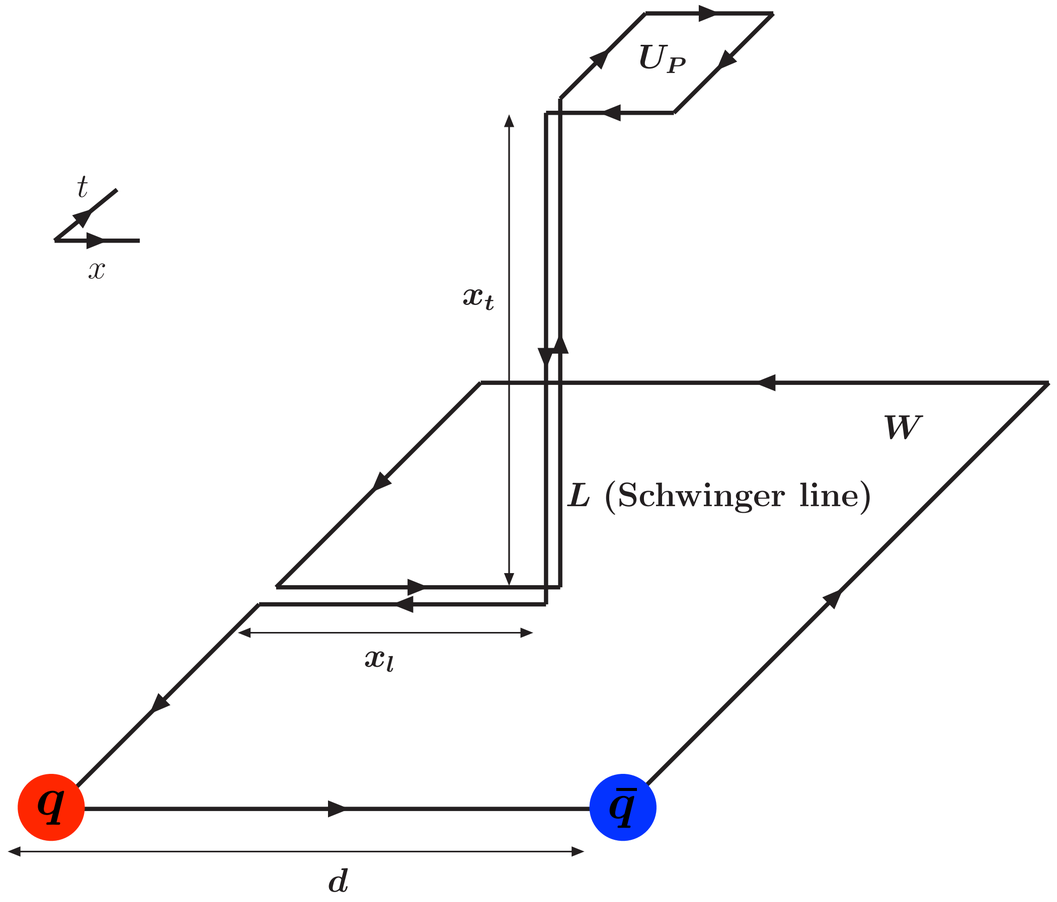

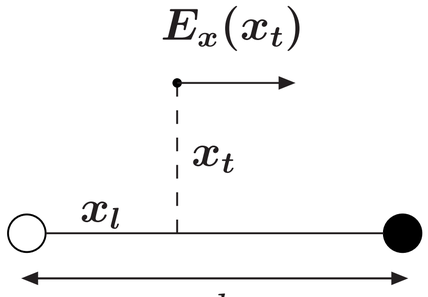

- **lattice measurements of the connected correlation function**

$$\rho^{\text{conn}}_{\mathbf{W},\mu\nu} = \frac{\langle \text{tr}(\mathbf{W L U_P L}^\dagger)\rangle}{\langle \text{tr}(\mathbf{W})\rangle} - \frac{\mathbf{1}}{\mathbf{N}} \frac{\langle \text{tr}(\mathbf{U_P})\text{tr}(\mathbf{W})\rangle}{\langle \text{tr}(\mathbf{W})\rangle}$$

- lattice definition of the **gauge-invariant field strength tensor**

$$\rho^{\text{conn}}_{\mathbf{W},\mu\nu} \equiv \mathbf{a^2 g}\langle \mathbf{F}_{\mu\nu}\rangle_{\mathbf{q\bar{q}}} \equiv \mathbf{a^2 g}\ \mathbf{F}_{\mu\nu}$$

- rotating the plaquette relative to the plane of the Wilson loop allows us to extract the **components of the field tensor:**
  - plaquette U_P in the plane $(\hat{\mu}=4,\hat{\nu}=1) \longrightarrow E_x$
  - plaquette U_P in the plane $(\hat{\mu}=4,\hat{\nu}=2) \longrightarrow E_y$
  - plaquette U_P in the plane $(\hat{\mu}=4,\hat{\nu}=3) \longrightarrow E_z$
  - plaquette U_P in the plane $(\hat{\mu}=2,\hat{\nu}=3) \longrightarrow B_x$
  - plaquette U_P in the plane $(\hat{\mu}=3,\hat{\nu}=1) \longrightarrow B_y$
  - plaquette U_P in the plane $(\hat{\mu}=4,\hat{\nu}=2) \longrightarrow B_z$

SYMMETRY: The fields take on the same values at spatial points connected by rotations around the axis on which the sources are located

Our earliest investigations

$$\rho^{\text{conn}}_{W,\mu\nu} \equiv \quad a^2 g \langle F_{\mu\nu} \rangle_{q\bar{q}} \quad \equiv \quad a^2 g \, F_{\mu\nu}$$

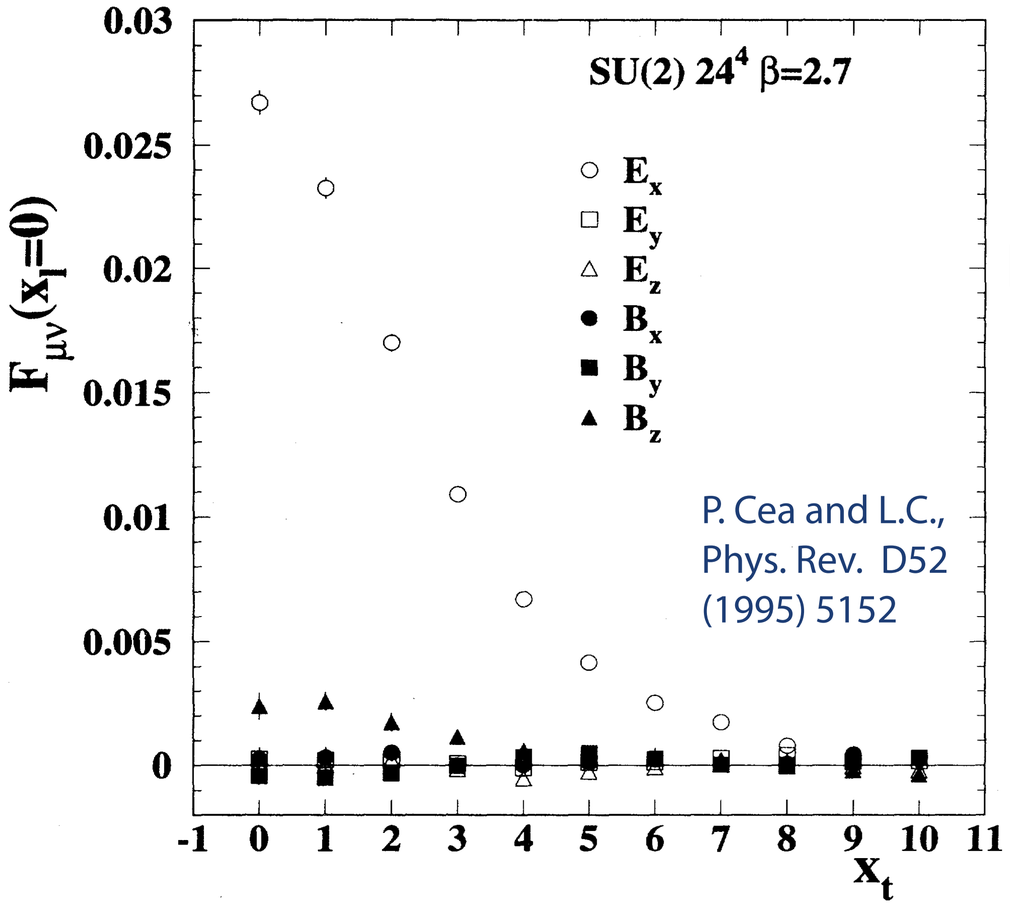

FIG. 2. The field strength tensor $F_{\mu\nu}(x_l, x_t)$ evaluated at $x_l = 0$ on a 24^4 lattice at $\beta = 2.7$, using Wilson loops of size 10×10 in Eq. (2.1).

The flux tube is almost completely formed by the longitudinal chromoelectric field.

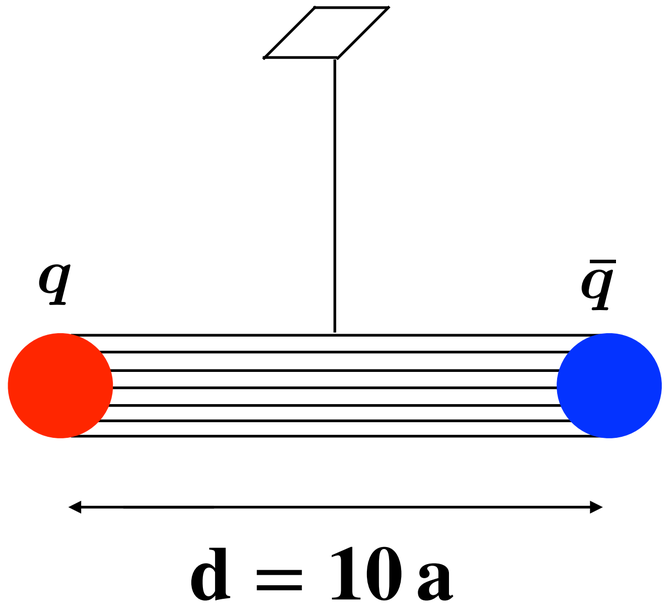

Systematic study of flux tubes in the case of:

- SU(3) pure gauge theory at $T = 0$
- SU(3) pure gauge theory at $T \neq 0$
- QCD with (2+1) HISQ flavors at $T = 0, \quad m_\pi = 160\ \mathrm{MeV}$
- QCD with (2+1) HISQ flavors with $m_\pi = 140\ \mathrm{MeV}$

  Preliminary results at $T \neq 0$

SU(3) T = 0 48^4 lattice $\beta = 6.240$ d = 1.14 fm

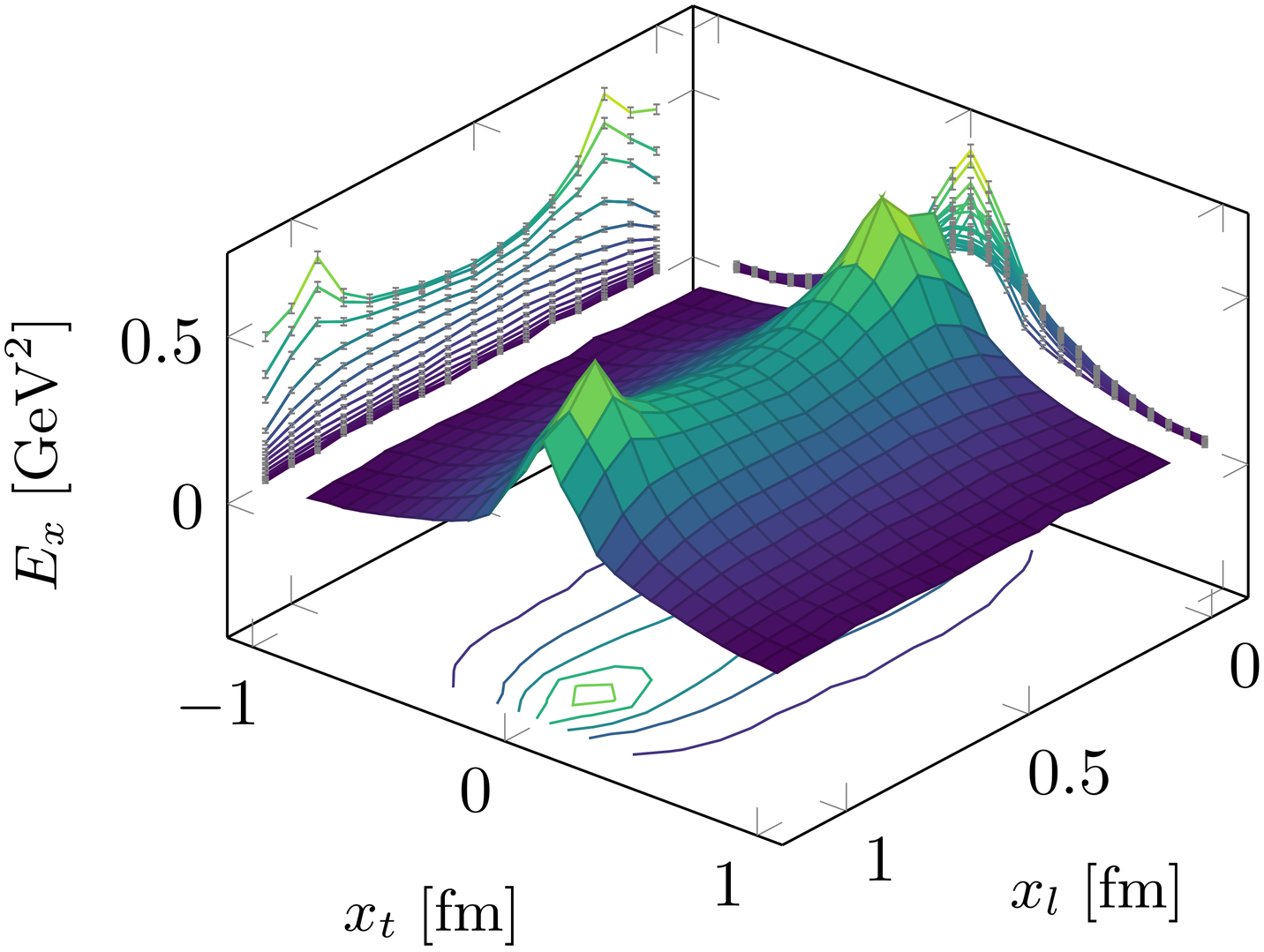

Full profile of the chromoelectric longitudinal field

$E_x(x_t, x_l)$

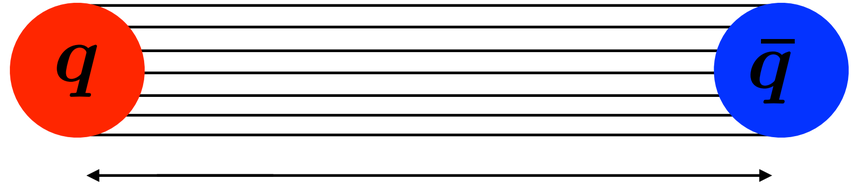

d = 1.14 fm

[M. Baker, P. Cea, V. Chelnolov, L.C., F. Cuteri, A. Papa, arXiv:1810.07133, arXiv:1912.04739]

SU(3) T = 0 → The chromoelectromagnetic field tensor

$E_x(x_t, x_l)$

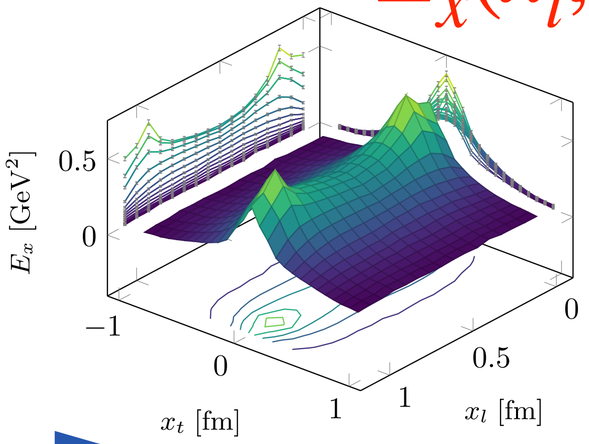

$E_y(x_t, x_l)$

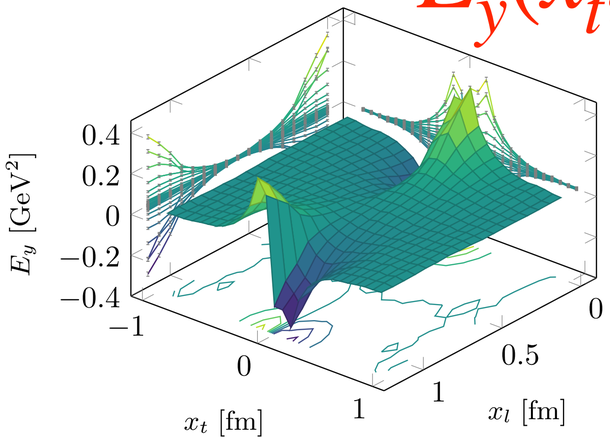

$E_z(x_t, x_l)$

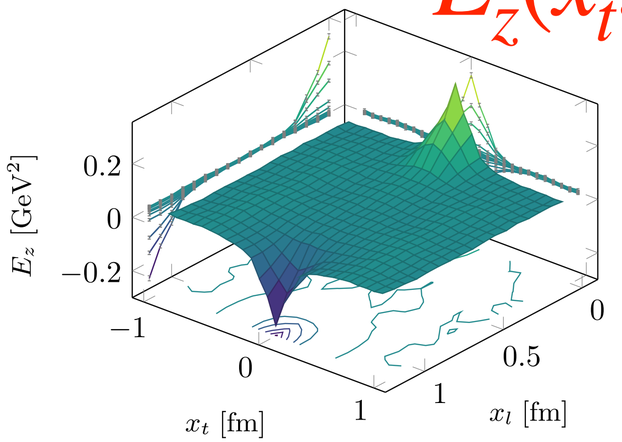

The chromomagnetic field around the sources is compatible with zero within statistical errors.

$B_x(x_t, x_l)$

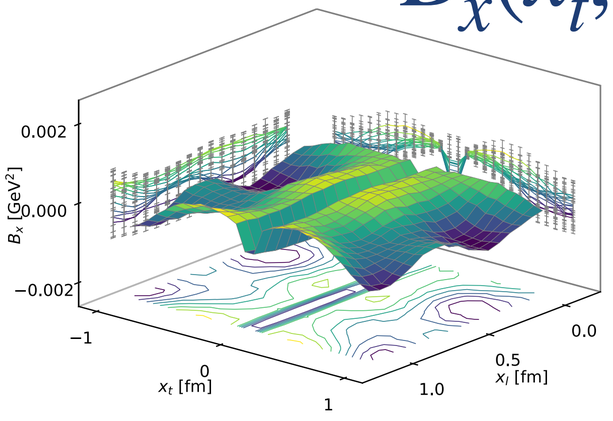

$B_y(x_t, x_l)$

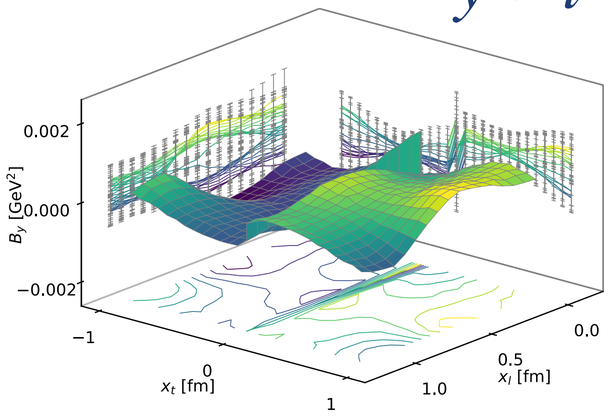

$B_z(x_t, x_l)$

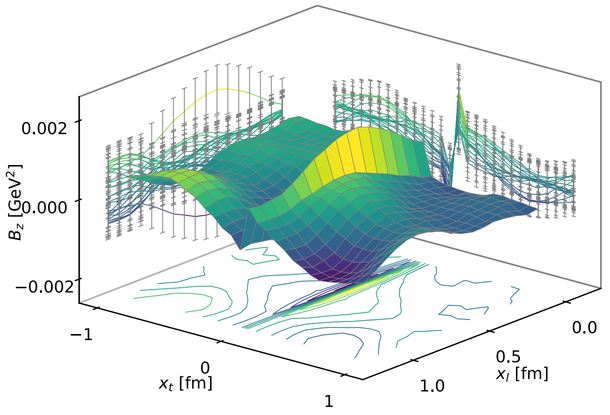

48^4 lattice $\beta = 6.240$ d = 1.14 fm

[M. Baker, P. Cea, V. Chelnolov, L.C., F. Cuteri, A. Papa, arXiv:1810.07133, arXiv:1912.04739]

SU(3)

$\beta = 6.370 \quad d = 0.85$ fm

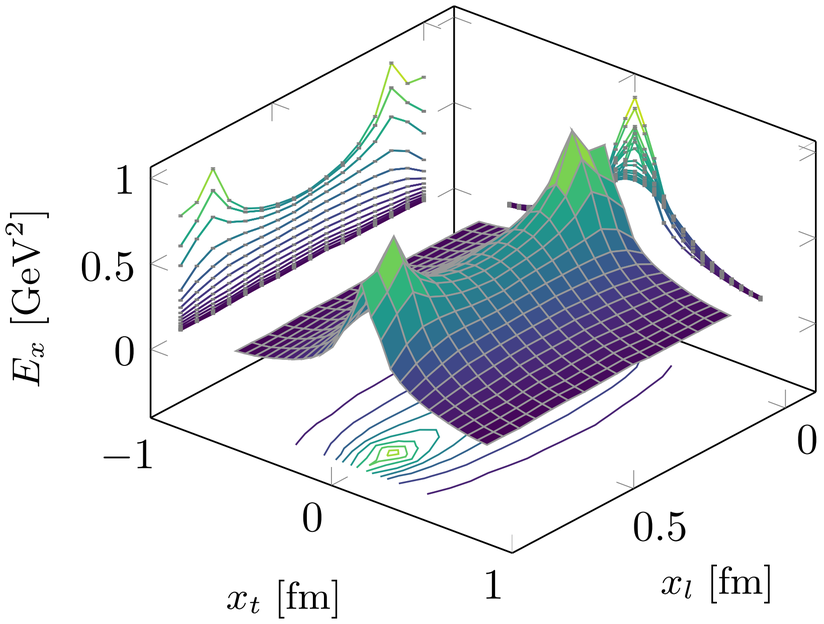

The dominant component of the chromoelectric field is longitudinal.

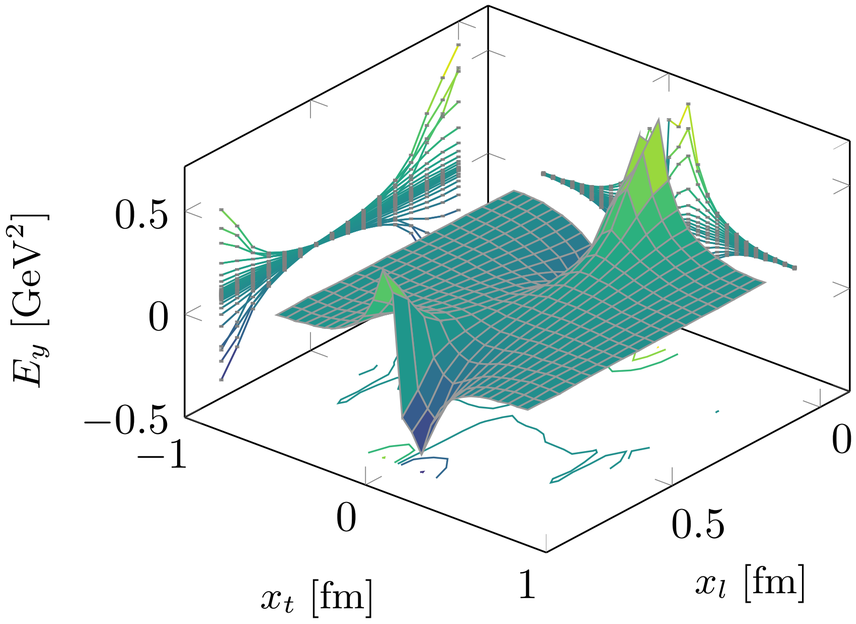

The components of the chromoelectric field transverse to the line connecting the sources can be matched to an effective Coulomb-like field.

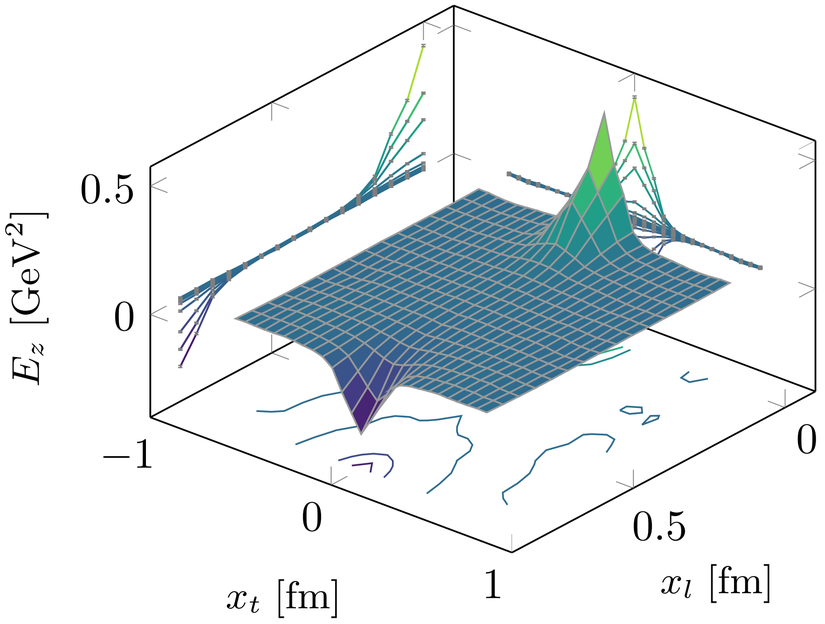

[M. Baker, P. Cea, V. Chelnolov, L.C., F. Cuteri, A. Papa, arXiv:1810.07133, arXiv:1912.04739]

Transverse chromoelectric components: effective Coulomb-like field

The components of the chromoelectric field transverse to the line connecting the sources can be matched to an effective Coulomb-like field $\vec{\mathbf{E}}^{\mathbf{C}}(\vec{\mathbf{r}})$ satisfying the following conditions:

- The transverse component $\mathbf{E_y}$ of the chromoelectric field is identified with the transverse component $\mathbf{E_y^C}$ of the perturbative field:

$$\mathbf{E_y^C} \equiv \mathbf{E_y}$$

- The perturbative field $\mathbf{E^C}$ is irrotational: $\vec{\nabla} \times \vec{\mathbf{E}}^{\mathbf{C}} = \mathbf{0}$

COMPUTE THE COULOMB-LIKE CONTRIBUTION IN A MODEL-INDEPENDENT WAY

The lattice procedure to evaluate the perturbative Coulomb-like contribution to the longitudinal chromoelectric field

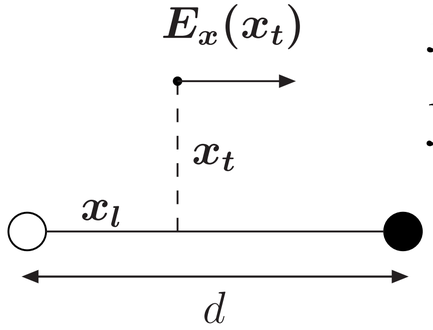

$$x \equiv x_l$$
$$y \equiv x_t$$

The irrotational condition on a discrete lattice (on a plaquette):

$$E_x^{\mathrm{C}}(x,y) + E_y^{\mathrm{C}}(x+1,y) - E_x^{\mathrm{C}}(x,y+1) - E_y^{\mathrm{C}}(x,y) = 0$$

Solve this equation for E_x^C

$$E_x^{\mathrm{C}}(x,y) = \sum_{y'=y}^{y_{\max}} \left(E_y(x,y') - E_y(x+1,y')\right) + E_x^{\mathrm{C}}(x, y_{\max}+1)$$

We further assume: $E_x^{\mathrm{C}}(x, y_{\max}+1) = 0$

The confining field of the QCD flux tube

$SU(3)\quad \beta = 6.370 \quad d = 16a = 0.85\ \text{fm}$ (*)

EXTRACT THE NONPERTURBATIVE CHROMOELECTRIC FIELD

The longitudinal $\mathbf{E_x}$ can be separated into the **perturbative**, short-distance part $\mathbf{E_x^C}$ and a **non perturbative** term $\mathbf{E_x^{NP}}$, encoding the confining information, which is shaped as a **smooth flux tube**.

$$\mathbf{E_x^{NP} = E_x - E_x^C}$$

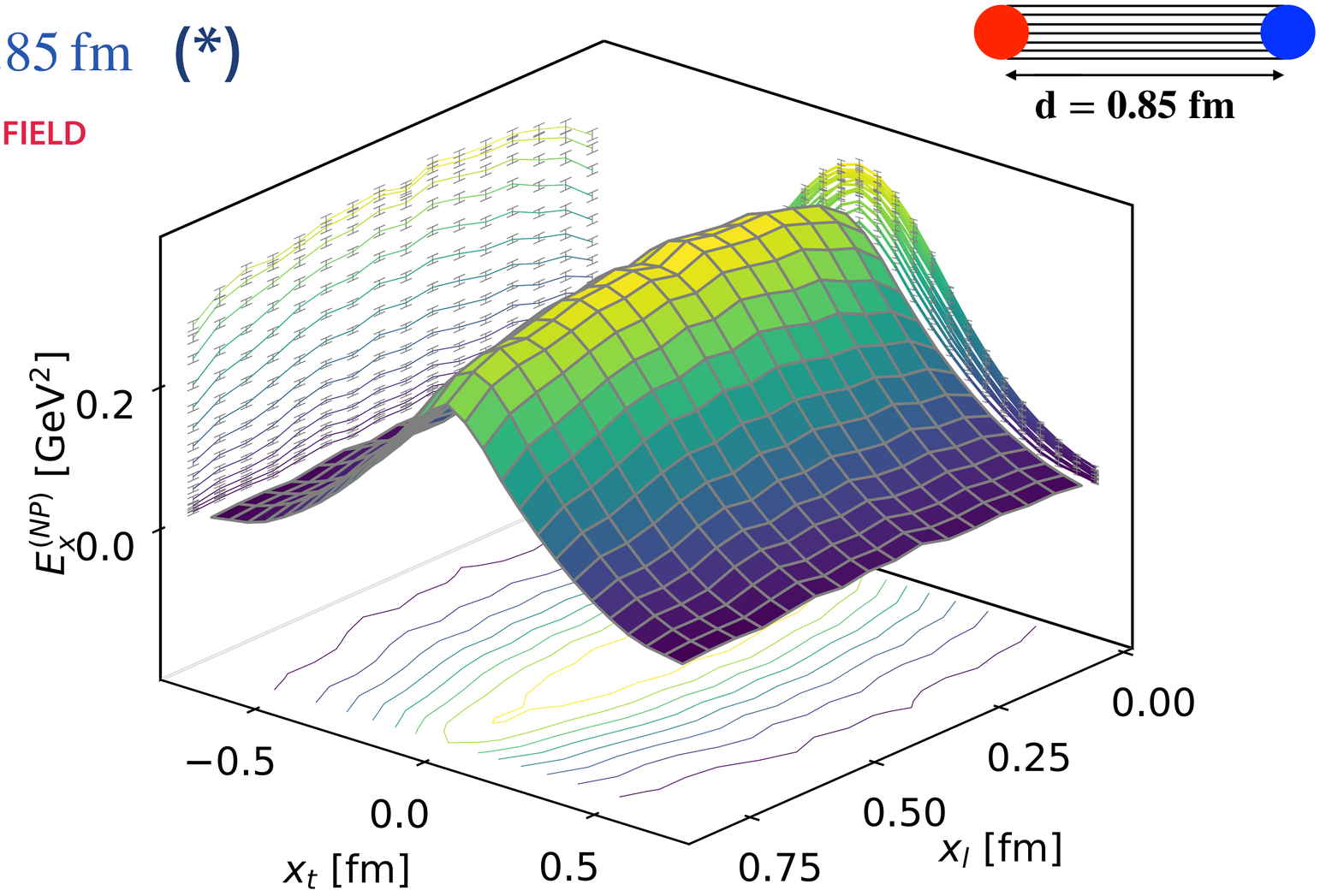

(*) **Lattice scale:**

$a(\beta) = r_0 \times \exp\left[c_0 + c_1(\beta-6) + c_2(\beta-6)^2 + c_3(\beta-6)^3\right]$

$r_0 = 0.5\ \text{fm}$

$c_0 = -1.6804\,, c_1 = -1.7331$

$c_2 = 0.7849\,, c_3 = -0.4428$

[S. Necco, R. Sommer, arXiv:hep-lat/0108008]

SU(3) $T \neq 0$

M. Baker, V. Chelnokov, L. Cosmai, F. Cuteri and A. Papa, [arXiv:2310.04298 [hep-lat]].

Measuring the chromoelectric fields within a flux tube generated by a static quark-antiquark pair in finite-temperature SU(3) gauge theory.

Table 1 Summary of the numerical simulations

Lattice	β	$a(\beta)$ [fm]	d/a	d [fm]	T/T_c	Statistics
$48^3 \times 12$	6.100	0.0789097	12	0.946917	0.8	2400
$48^3 \times 12$	6.381	0.052633	12	0.631597	1.2	340
$48^3 \times 12$	6.381	0.052633	16	0.842129	1.2	1500
$48^3 \times 12$	6.554	0.0420845	15	0.631267	1.5	1100
$32^3 \times 8$	6.248	0.0631757	10	0.631757	1.5	2580
$48^3 \times 12$	6.778	0.0315769	20	0.631537	2.0	1020

SCALING ANALYSYS

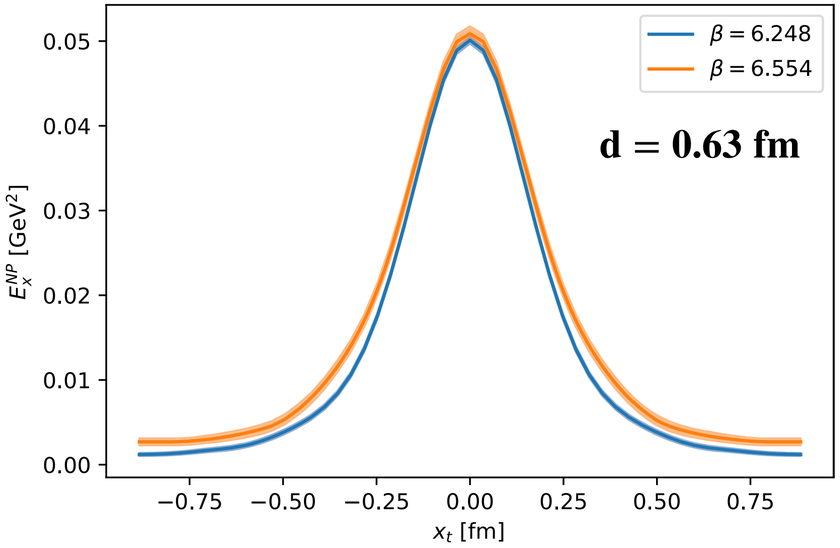

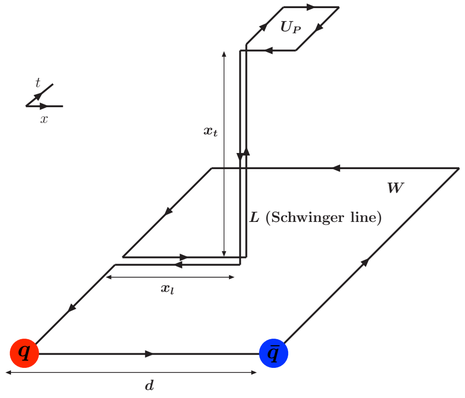

$$T = \frac{1}{a(\beta)\, N_t} \qquad T_c = 260\,\text{MeV}$$

Measurement of the chromoelectric field using the maximal Wilson loop (i.e. the loop with the largest possible extension in the temporal direction).

O. Jahn, O. Philipsen, Phys. Rev. D 70, 074504 (2004). arxiv:hep-lat/0407042

e.g.: lattice $48^3 \times 12$ and distance $d = 15a$ between the sources —> Wilson loop $15(\text{space}) \times 12(\text{time})$

The nonperturbative chromoelectric field

Full profile of the chromoelectric field

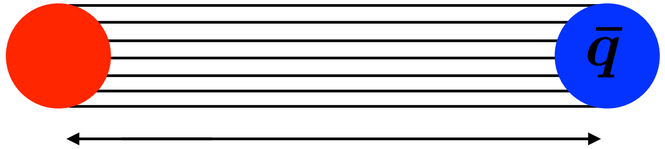

$\mathbf{d = 0.631\ fm}$

SU(3) $T \neq 0$

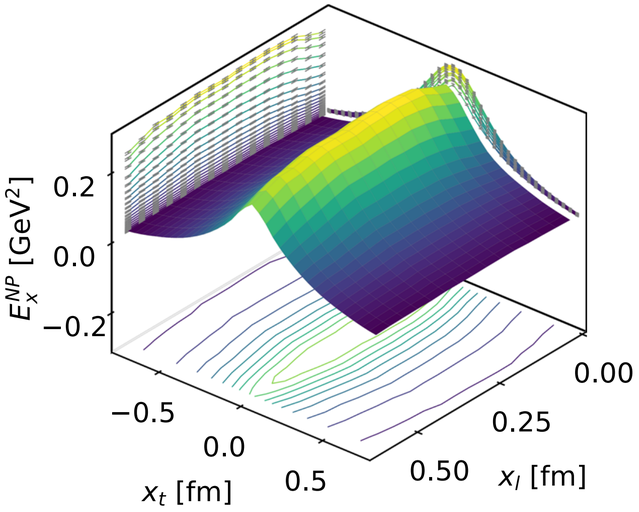

$\mathbf{T = 0}$

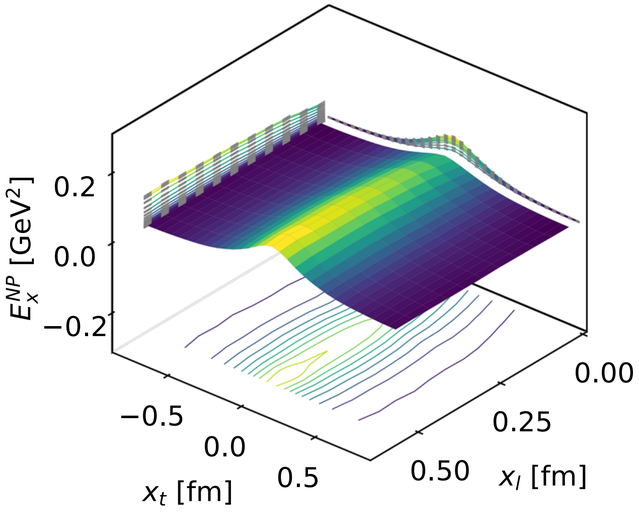

$\mathbf{T = 1.2\,T_c}$

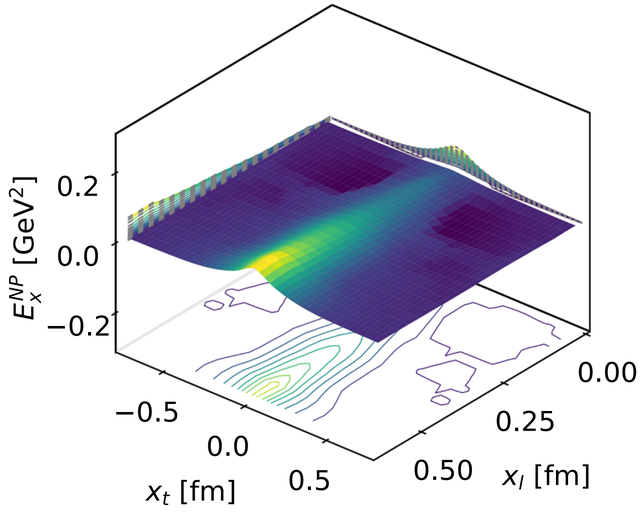

$\mathbf{T = 2.0\,T_c}$

The chromoelectric field continues to form a tube-like structure well after reaching the deconfinement temperature, despite the values becoming much smaller at higher temperatures.

The chromoelectric field at the midplane between the sources

SU(3) $T \neq 0$

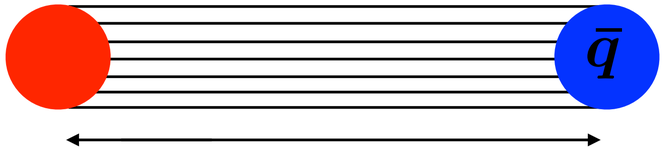

$\mathbf{d = 0.632\ fm}$

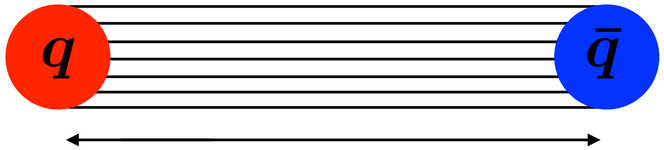

$\mathbf{d = 0.632\ fm\ ,\quad d = 0.842\ fm}$

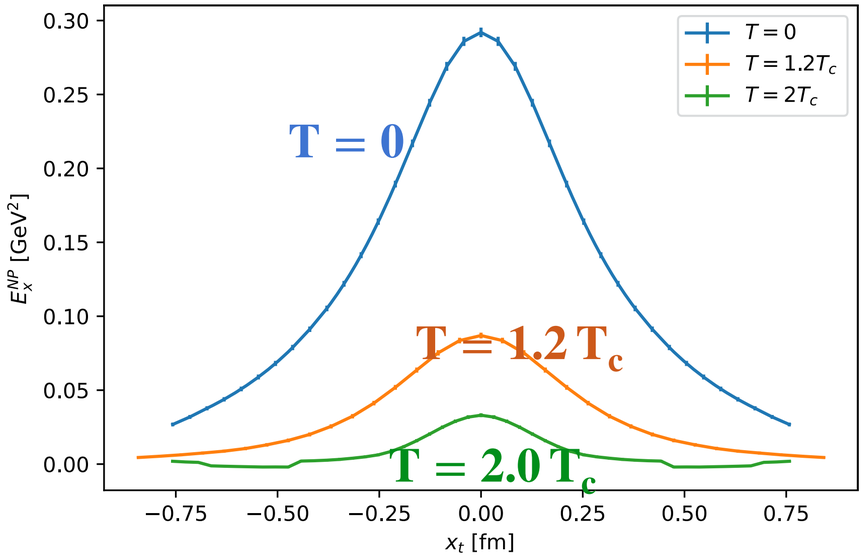

The non perturbative chromoelectric field at the midplane: providing a better view of the flux-tube remnant evaporation at $T > T_c$

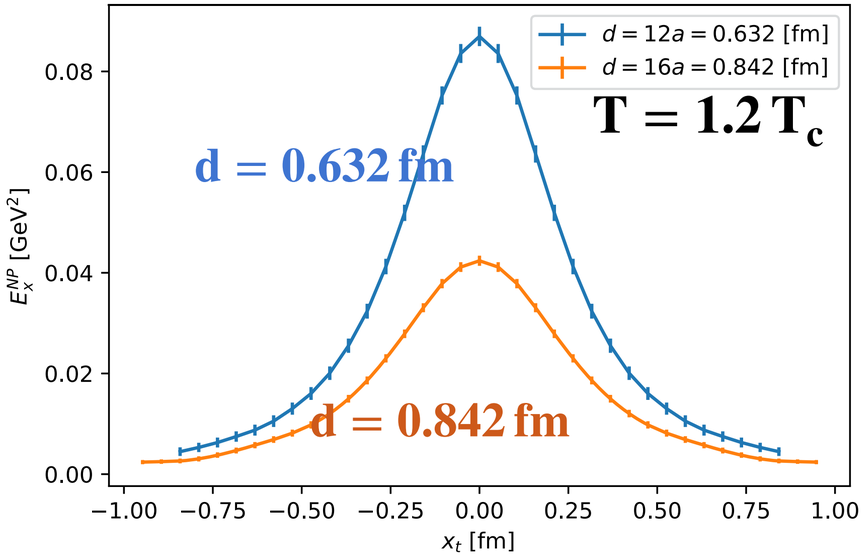

When the quark-antiquark separation is increased by 1/3, the field values fall by more than 50%, and thus the flux-tube remnant does not create a linear potential at large distances.

The effective string tension

SU(3) $T \neq 0$

$$\sigma_{\text{eff}} = \int d^2 x_t \, \frac{(E_x^{NP}(x_t))^2}{2}$$

numerical evaluation of the integral using the data for the nonperturbative chromoelectric field at the midplane

β	d [fm]	T/T_c	$\sqrt{\sigma_{\text{eff}}}$ [GeV]
6.240	0.511	0	0.4742(15)
6.544	0.511	0	0.4692(23)
6.769	0.511	0	0.467(7)
6.554	0.631	0	0.487(6)
6.100	0.947	0.8	0.535(20)
6.381	0.632	1.2	0.129(4)
6.381	0.842	1.2	0.0733(25)
6.554	0.631	1.5	0.0625(19)
6.248	0.632	1.5	0.0556(8)
6.778	0.632	2.0	0.0305(14)

$T < T_c$ → $\sqrt{\sigma_{\text{eff}}}$ remains almost constant as the separation distance d between the sources increases.

$T > T_c$ → $\sqrt{\sigma_{\text{eff}}}$ decreases with increasing temperature T or with increasing separation distance d between the sources.

QCD (2+1) HISQ flavors at $T = 0$

LATTICE SETUP

- Simulation of lattice **QCD with 2+1 flavors of HISQ (Highly Improved Staggered Quarks) quarks**, with the tree-level improved Symanzik gauge action (HISQ/tree).

- Couplings are adjusted so as to move on a **line of constant physics** (LCP), as determined in Bazavov et al (arXiv:111.1710) with the strange quark mass m_s fixed at its physical value and a light-to-strange mass ratio $m_l/m_s = 1/20$, corresponding to a **pion mass of 160 MeV** in the continuum limit.

- We fix the **lattice spacing** through the observable r_1 as defined in Bazavov et al (arXiv:111.1710)

$$\frac{a}{r_1}(\beta)_{m_l=0.05m_s} = \frac{c_0 f(\beta) + c_2(10/\beta) f^3(\beta)}{1 + d_2(10/\beta) f^2(\beta)}$$

$$c_0 = 44.06,\ c_2 = 272102,\ d_2 = 4281,\ r_1 = 0.3106(20)\ \text{fm}$$

- **MILC code** for producing **gauge configurations** (1 saved after 25 RHMC trajectories) and for the measurements of the chromoelectromagnetic field tensor. **Simulations on LEONARDO@Cineca.**

- **Smoothing of gauge configuration:** 1HYP on temporal links + n HYP3d on space links.

SUMMARY OF THE NUMERICAL SIMULATIONS

lattice size	beta	a(beta) [fm]	d [lattice spacings]	d [fm]	#of measurements
48^4	6.885	0.0949777	6	0.569866	500
32^4	7.158	0.0738309	8	0.590647	10064
24^4	6.445	0.144692	5	0.723462	3330
32^4	7.158	0.0738309	10	0.738309	10181
48^4	6.885	0.0949777	8	0.75982	779
32^4	6.885	0.0949777	8	0.759821	4409
32^4	6.5824	0.126658	6	0.759947	2667
32^4	6.3942	0.15203	5	0.760151	3000
32^4	6.885	0.0949777	9	0.854799	4347
32^4	6.25765	0.173715	5	0.868573	3545
32^4	6.5824	0.126658	7	0.886605	2667
32^4	6.3942	0.15203	6	0.912182	3000
48^4	6.885	0.0949777	10	0.949777	779
32^4	7.158	0.0738309	13	0.959801	10183
24^4	6.445	0.144692	7	1.01285	3330
32^4	6.5824	0.126658	8	1.01326	2666
32^4	7.158	0.0738309	14	1.03363	2107
32^4	6.25765	0.173715	6	1.04229	3549
32^4	6.885	0.0949777	11	1.04475	4408
32^4	6.3942	0.15203	7	1.06421	3000
32^4	6.33727	0.160714	7	1.125	3133
32^4	6.885	0.0949777	12	1.13973	4409
48^4	6.885	0.0949777	12	1.13973	769
32^4	6.5824	0.126658	9	1.13992	2667
32^4	6.314762	0.164286	7	1.15	3651
24^4	6.445	0.144692	8	1.157536	3330
32^4	6.28581	0.168999	7	1.18299	3148
32^4	6.25765	0.173715	7	1.216	3546
32^4	6.3942	0.15203	8	1.21624	3000
32^4	6.885	0.0949777	13	1.23471	4409
32^4	6.5824	0.126658	10	1.26658	2667
32^4	6.3942	0.15203	9	1.36827	3000

- **distance between the static sources:**

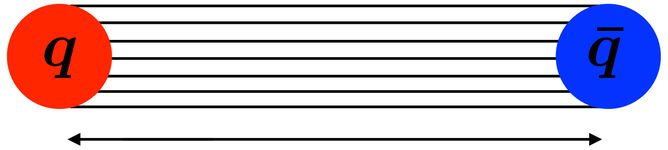

$$0.570 \leq d \leq 1.368 \text{ fm}$$

$$\rho^{\text{conn}}_{W,\mu\nu}$$

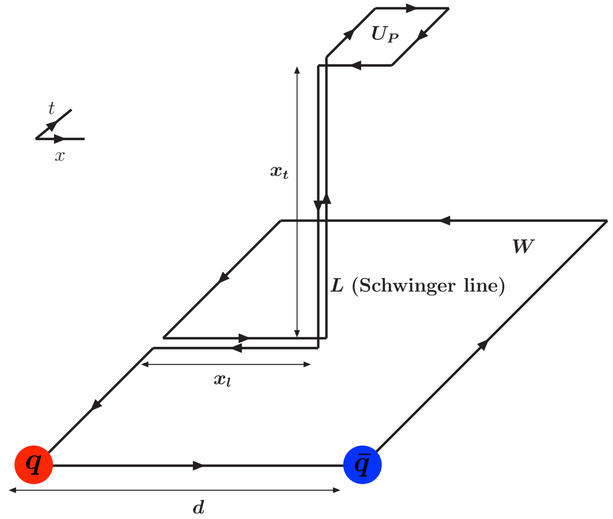

- **Nontrivial renormalization** [N.Battelli, C.Bonati, arXiv:1903.10463] which depends on $\mathbf{x_t}$.
  By comparing our results we argued that **smearing** behaves as an **effective renormalization.**
- The smearing procedure can also be validated a posteriori by the **observation of continuum scaling.**

CONTINUUM SCALING

$0.855\ \text{fm} \leq d \leq 0.959\ \text{fm}$

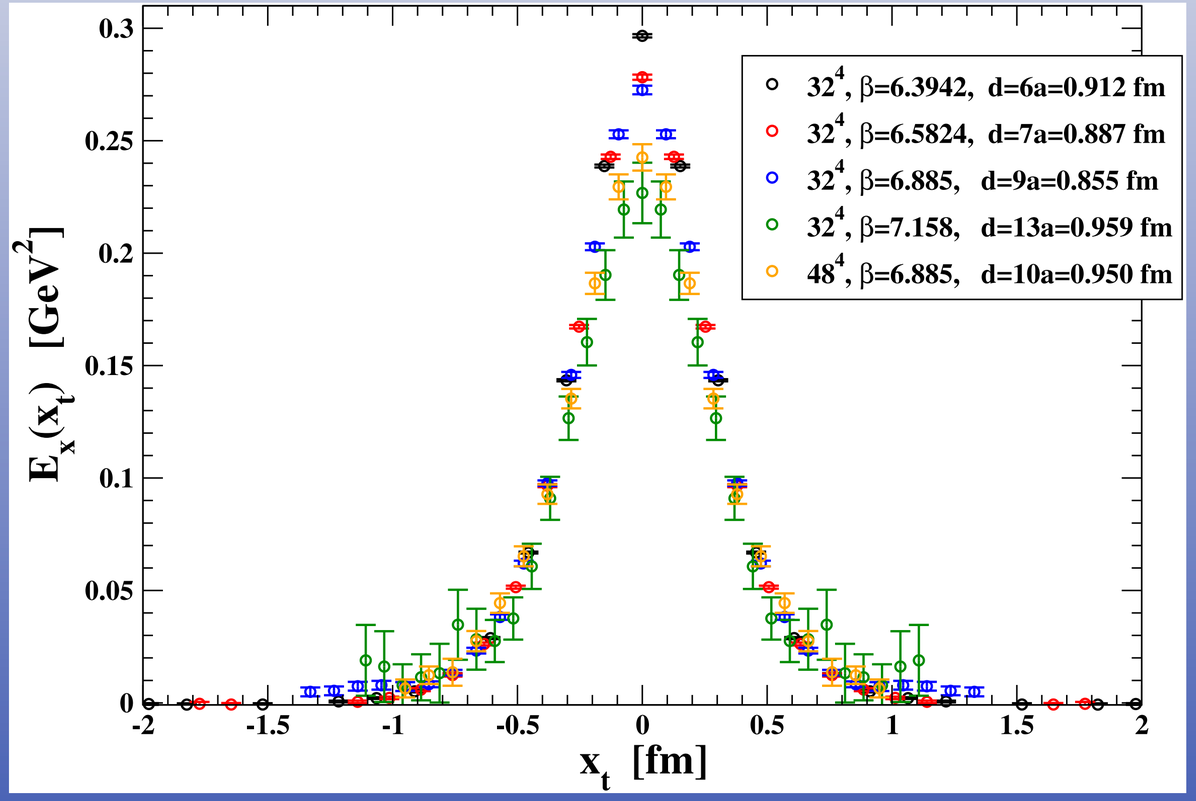

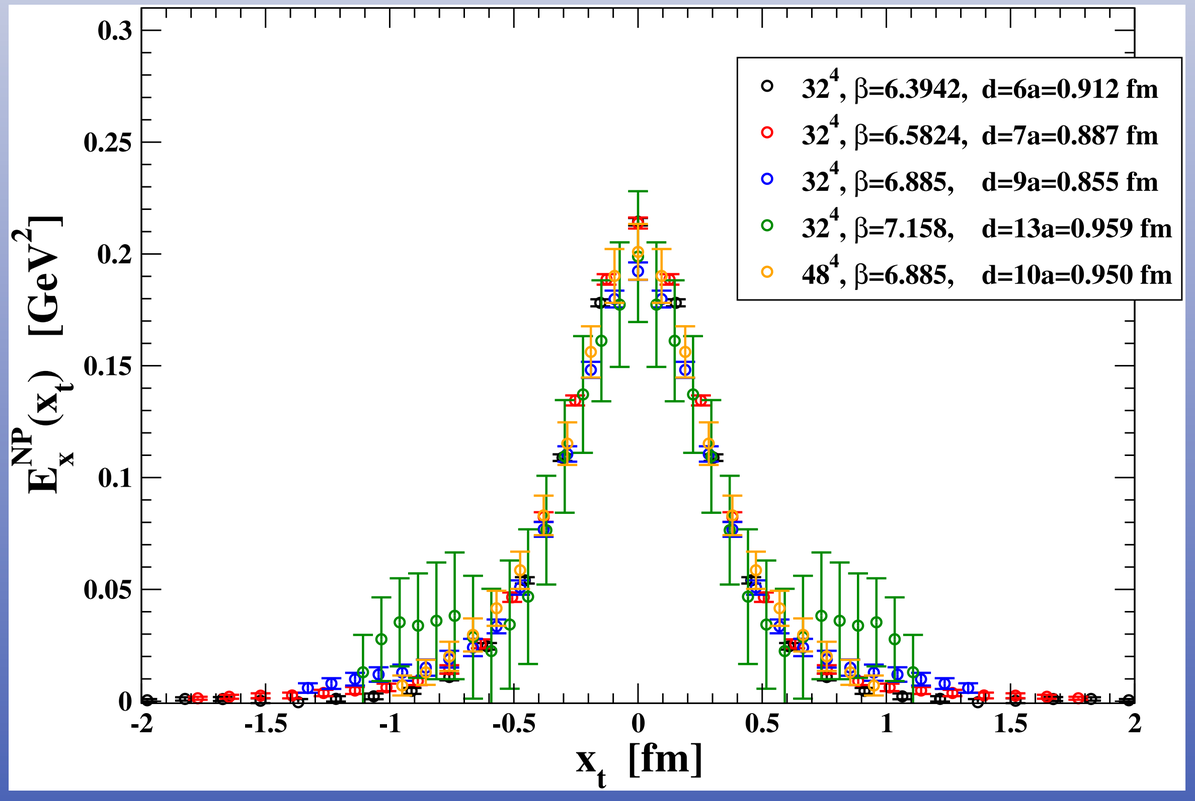

QCD (2+1) flavors: longitudinal chromoelectric field

$\beta = 7.158 \quad d = 10a = 0.74 \ \text{fm}$

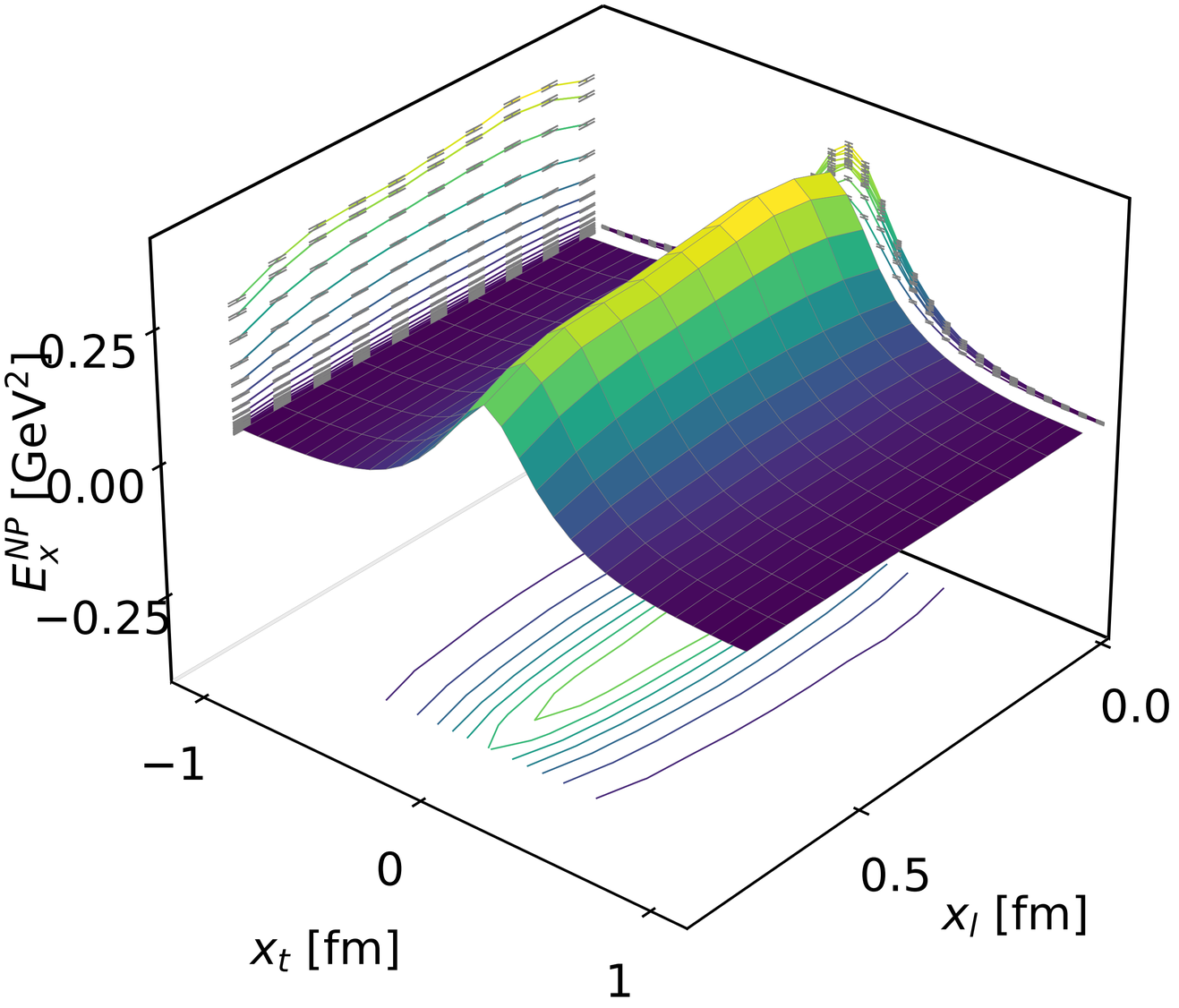

at midplane

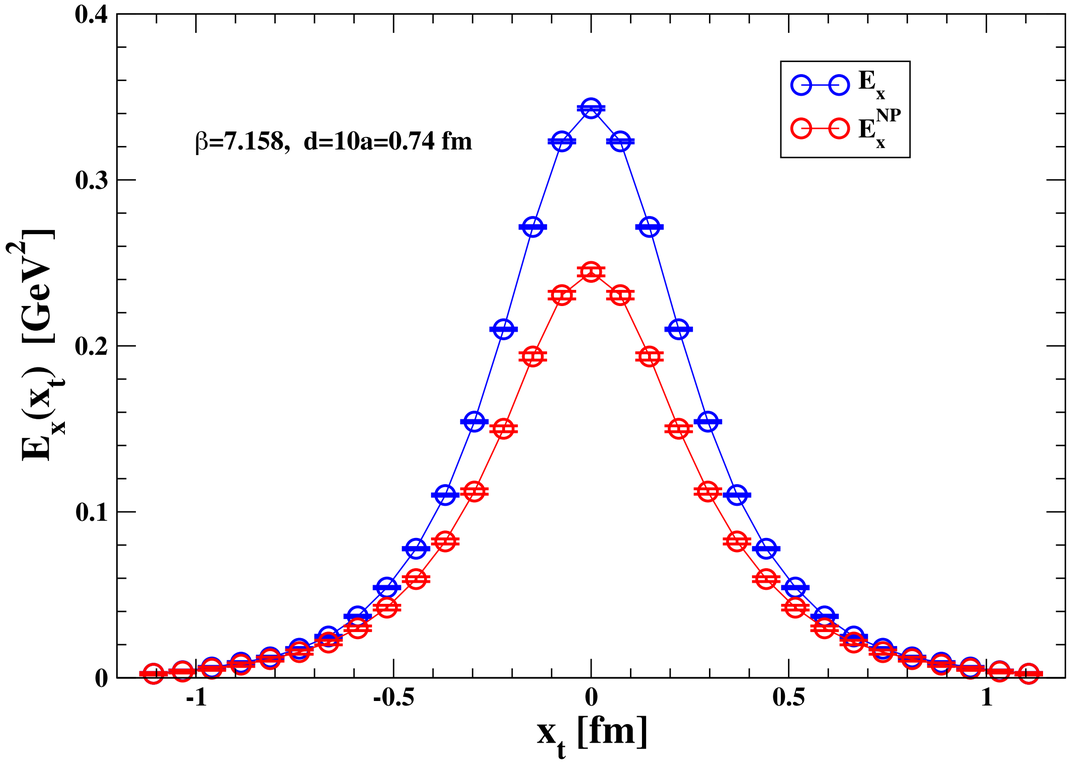

EFFECTIVE STRING TENSION

To characterize quantitatively the **shape** and some **properties of the flux tube** formed by the longitudinal electric field, we calculated numerically (at the midplane between the sources):

$$\sigma_{\rm eff} = \int d^2x_t \, \frac{(E_x^{\rm NP}(x_t))^2}{2}$$

"effective" string tension

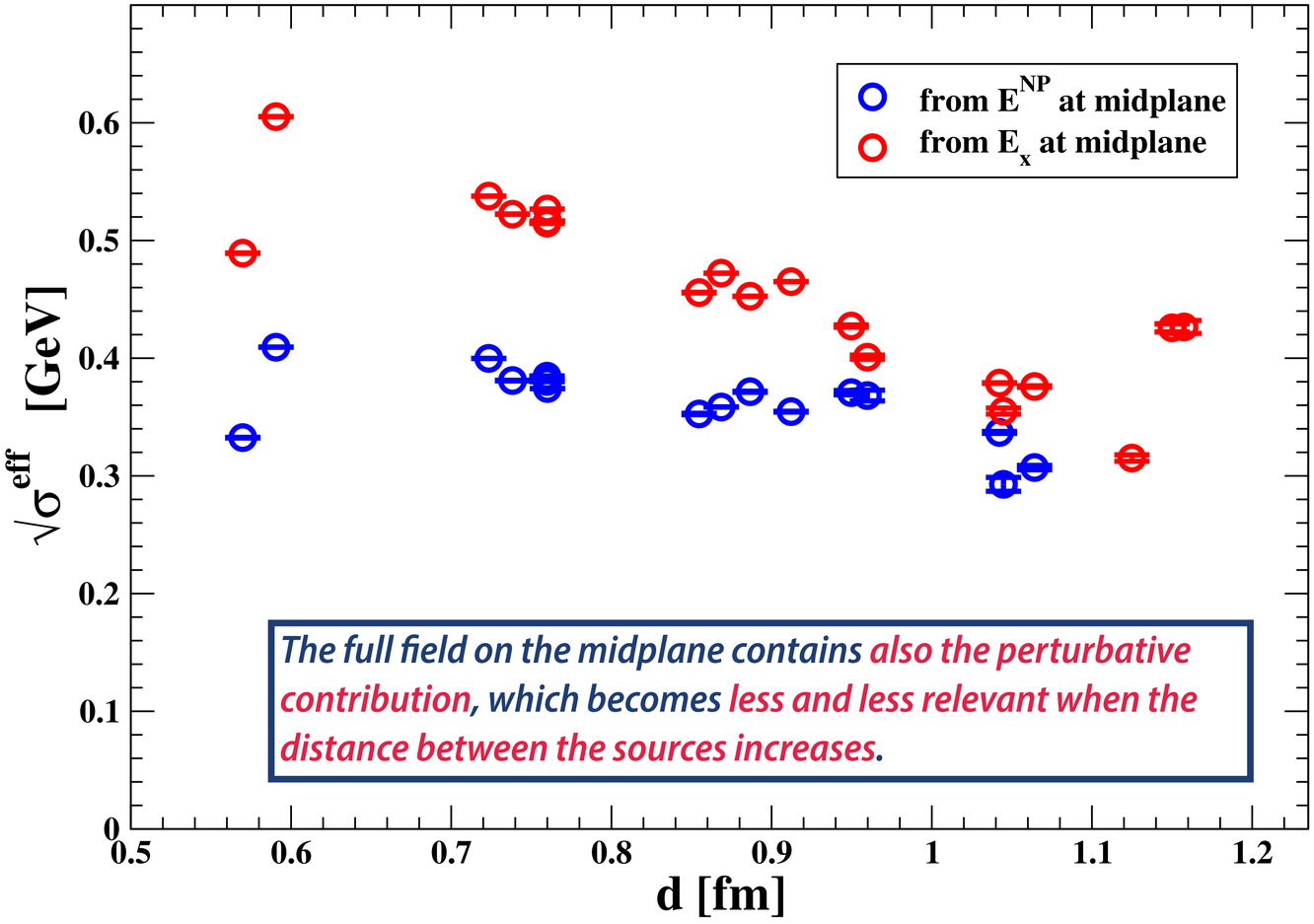

The full field on the midplane contains also the perturbative contribution, which becomes less and less relevant when the distance between the sources increases.

E_x^{NP} at the midplane

d [fm]	$\sqrt{\sigma_{\rm eff}}$
0.569866	0.429194 (274)
0.590647	0.528448 (75)
0.723462	0.516102 (99)
0.738309	0.491825 (329)
0.759820	0.496651 (241)
0.759821	0.490815 (265)
0.759947	0.493505 (151)
0.760151	0.483090 (88)
0.854799	0.455193 (822)
0.868575	0.462862 (151)
0.886605	0.479558 (580)
0.912182	0.457725 (412)
0.949777	0.478554 (2312)
0.959801	0.475391 (5830)
1.042290	0.434895 (1046)
1.044750	0.377955 (7626)
1.064210	0.396417 (2382)

E_x at the midplane

d [fm]	$\sqrt{\sigma_{\rm eff}}$
0.569866	0.631414 (229)
0.590647	0.781308 (43)
0.723462	0.693967 (59)
0.738309	0.674144 (165)
0.759820	0.664316 (146)
0.759821	0.665628 (129)
0.759947	0.679893 (68)
0.760151	0.667025 (41)
0.854799	0.588196 (364)
0.868575	0.609614 (66)
0.886605	0.584165 (219)
0.912182	0.600249 (160)
0.949777	0.551526 (1235)
0.959801	0.517467 (2268)
1.042290	0.488990 (350)
1.044750	0.458335 (3327)
1.064210	0.485249 (756)
1.125000	0.406767 (3461)
1.150000	0.549577 (4495)
1.157536	0.550451 (7072)

$$\sqrt{\sigma_{\rm eff}} \approx 0.45 \text{ GeV}$$

WIDTH OF THE FLUX TUBE

To characterize quantitatively the **shape** and some **properties of the flux tube** formed by the longitudinal electric field, we calculated numerically (at the midplane between the sources):

$$w = \sqrt{\frac{\int d^2x_t \, x_t^2 E_x^{NP}(x_t)}{\int d^2x_t \, E_x^{NP}(x_t)}}$$

width of the flux tube

$$w \approx 0.5 \text{ fm}$$

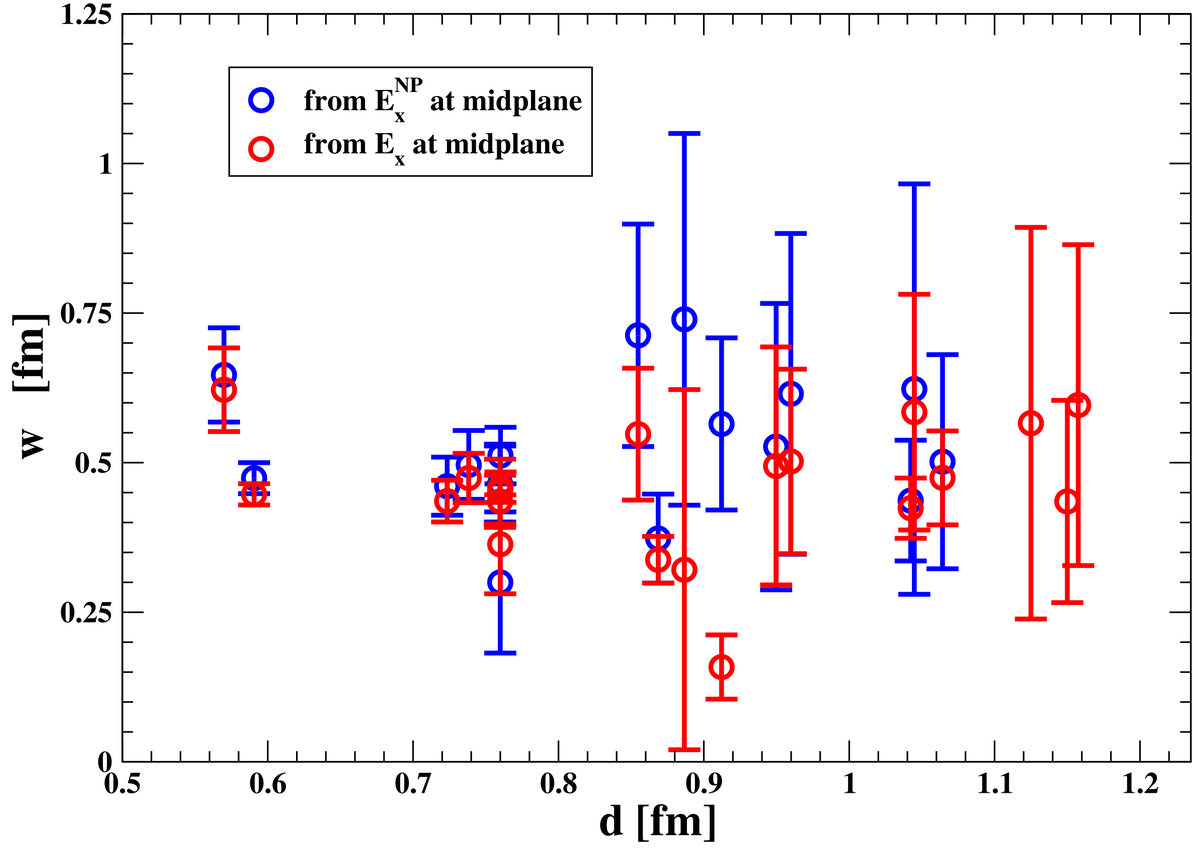

E_x^{NP} at the midplane

d [fm]	w
0.569866	0.646585 (78748)
0.590647	0.474086 (25839)
0.723462	0.460645 (48577)
0.738309	0.496320 (57512)
0.75982	0.463356 (67456)
0.759821	0.464393 (63411)
0.759947	0.299796 (117924)
0.760151	0.511873 (47241)
0.854799	0.712877 (185931)
0.868575	0.373149 (74361)
0.886605	0.739608 (310653)
0.912182	0.564672 (143845)
0.949777	0.526818 (239288)
0.959801	0.614954 (268025)
1.04229	0.436552 (100896)
1.04475	0.622952 (342927)
1.06421	0.501584 (178880)

E_x at the midplane

d [fm]	w
0.569866	0.621870(69886)
0.590647	0.447115(17753)
0.723462	0.435692(34762)
0.738309	0.474240(41283)
0.75982	0.451601(54312)
0.759821	0.435405(43580)
0.759947	0.363556(82688)
0.760151	0.459008(25524)
0.854799	0.547670(110240)
0.868575	0.337704(39088)
0.886605	0.321108(300997)
0.912182	0.158464(53710)
0.949777	0.494548(198891)
0.959801	0.502093(154215)
1.04229	0.423873(50377)
1.04475	0.584496(197020)
1.06421	0.474587(78494)
1.125	0.565908(327225)
1.15	0.435095(169046)
1.157536	0.596161(268178)

the width of the flux tube remains stable on a wide range of distances and is generally compatible for the full and the nonperturbative field.

POSSIBLE EVIDENCE FOR STRING BREAKING

We tried to push our numerical simulations to distances as large as ~ 1.37 fm, searching for **hints of string breaking**.

- $0.570 \text{ fm} \leq d \leq 1.064 \text{ fm}$

  We are able to isolate the nonperturbative part of the longitudinal electric field

- $1.140 \text{ fm} \lesssim d < 1.368 \text{ fm}$

  We find evidences for the full longitudinal electric field E_x on the midplane between two sources

  BUT

  there are not evidences for a sizeable nonperturbative longitudinal electric field E_x^{NP}.

- For $d > 1.140$ fm

  No improvement in the signal can be observed **if the distance in lattice units between the two sources is reduced**, **keeping d fixed.**

- In **SU(3) pure gauge**, where the string remains unbroken by definition, **the signal for the longitudinal field is clear even at large distances both in physical and lattice units**.

Our preliminary estimate for the string breaking distance is:

$$1.064 \text{ fm} \lesssim d^* \lesssim 1.140 \text{ fm}$$

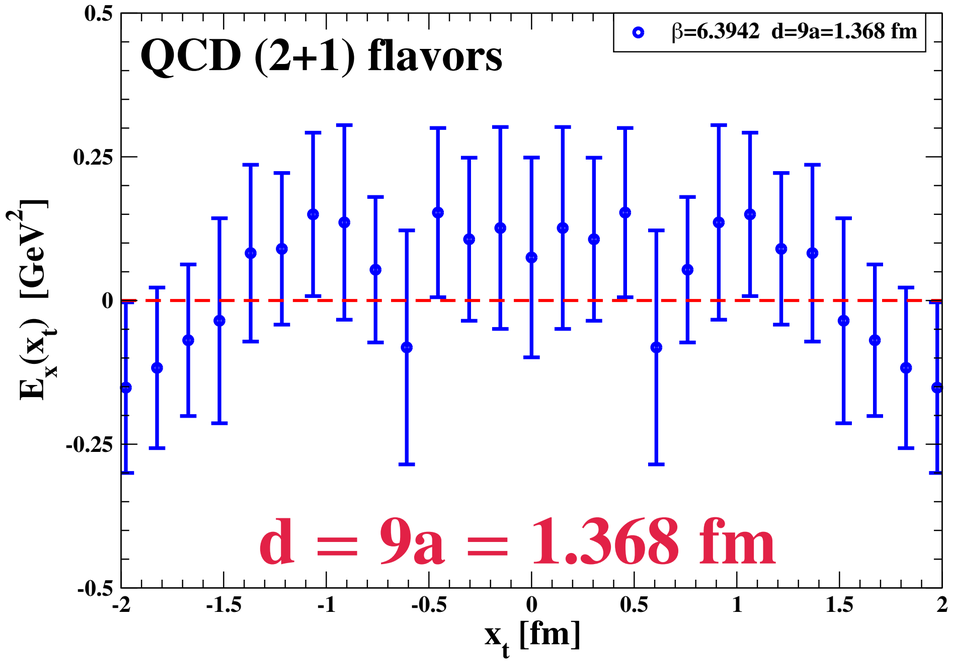

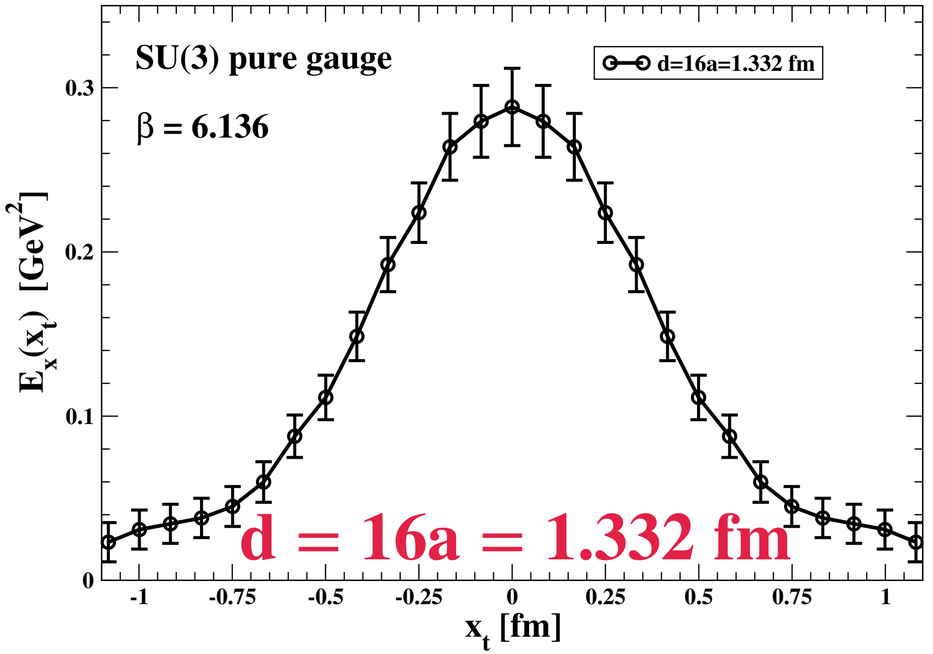

QCD (2+1) HISQ flavors at $T \neq 0$ $(m_\pi = 140\,\mathrm{MeV})$

LATTICE SETUP

- Simulation of lattice **QCD with 2+1 flavors of HISQ (Highly Improved Staggered Quarks) quarks**, with the tree-level improved Symanzik gauge action (HISQ/tree).

- Couplings are adjusted so as to move on a **line of constant physics** (LCP), as determined in Bazavov et al (arXiv:1701.04325) with the strange quark mass $\mathbf{m_s}$ fixed at its physical value and a light-to-strange mass ratio $\mathbf{m_l/m_s = 1/27}$, corresponding to a **pion mass of 140 MeV** in the continuum limit.

- We fix the **lattice spacing** through the observable $\mathbf{f_K}$ as defined in Bazavov et al (arXiv:111.1710)

$$\mathbf{a}(\beta) = \frac{\mathbf{r_1}}{\mathbf{r_1 f_K}} \frac{\mathbf{c_0^K f}(\beta) + \mathbf{c_2^K}(\mathbf{10}/\beta)\mathbf{f^3}(\beta)}{\mathbf{1} + \mathbf{d_2^K}(\mathbf{10}/\beta)\mathbf{f^2}(\beta)}$$

$$r_1 = 0.3106\ \mathrm{fm}$$

$$r_1 f_K = \frac{0.3106\ \mathrm{fm} \cdot 156.1/\sqrt{2}\ \mathrm{MeV}}{197.3\ \mathrm{MeV\ fm}}$$

$$c_0^K = 7.66\ ,\ c_2^K = 32911\ ,\ d_2^K = 2388$$

$$f(\beta) = [b_0(10/\beta)]^{-b_1/(2b_0^2)} \exp[-\beta/(20b_0)]$$

- **MILC code** for producing **gauge configurations** (1 saved after 25 RHMC trajectories) and for the measurements of the chromoelectromagnetic field tensor. **Simulations on LEONARDO@Cineca.**

- **Smoothing of gauge configuration:** 1HYP on temporal links + n HYP3d on space links.

QCD (2+1) HISQ flavors lattice configurations ($m_\pi = 140$ MeV)

lattice	$\beta = 10/g^2$	$a(\beta)$ [fm]	m_l	m_s	T [MeV]	configurations
48^4	6.880	0.096292	0.00153	0.0413	42.7	1692
$48^3 \times 16$	6.880	0.096292	0.00153	0.0413	128.1	6316
$48^3 \times 8$	6.200	0.192133	0.00324	0.0876	128.4	5041
$48^3 \times 12$	6.590	0.128142	0.00206	0.0556	128.3	5365
$48^3 \times 14$	6.745	0.109799	0.00175	0.0472	128.4	5186
$48^3 \times 14$	6.880	0.096292	0.00153	0.0413	146.4	3603
$48^3 \times 12$	6.880	0.096292	0.00153	0.0413	170.8	3712
$48^3 \times 10$	6.880	0.096292	0.00153	0.0413	204.9	8073
$48^3 \times 6$	6.371	0.160462	0.00264	0.0712	205.0	5063
$48^3 \times 8$	6.653	0.120284	0.00193	0.0520	205.1	5511
$48^3 \times 8$	6.880	0.096292	0.00153	0.0413	256.2	5041
$48^3 \times 6$	6.590	0.128142	0.00206	0.0556	256.7	5447
$48^3 \times 6$	6.880	0.096292	0.00153	0.0413	341.5	4716
$48^3 \times 8$	7.186	0.0722645	0.00114	0.0307	341.3	7789
$48^3 \times 4$	6.471	0.144669	0.00235	0.0634	341.0	7374
$48^3 \times 4$	6.880	0.096292	0.00153	0.0413	512.3	5424

43 MeV $\leq$ T $\leq$ 512 MeV

MEASUREMENT OF THE TENSOR FIELD GENERATED BY A QUARK-ANTIQUARK PAIR

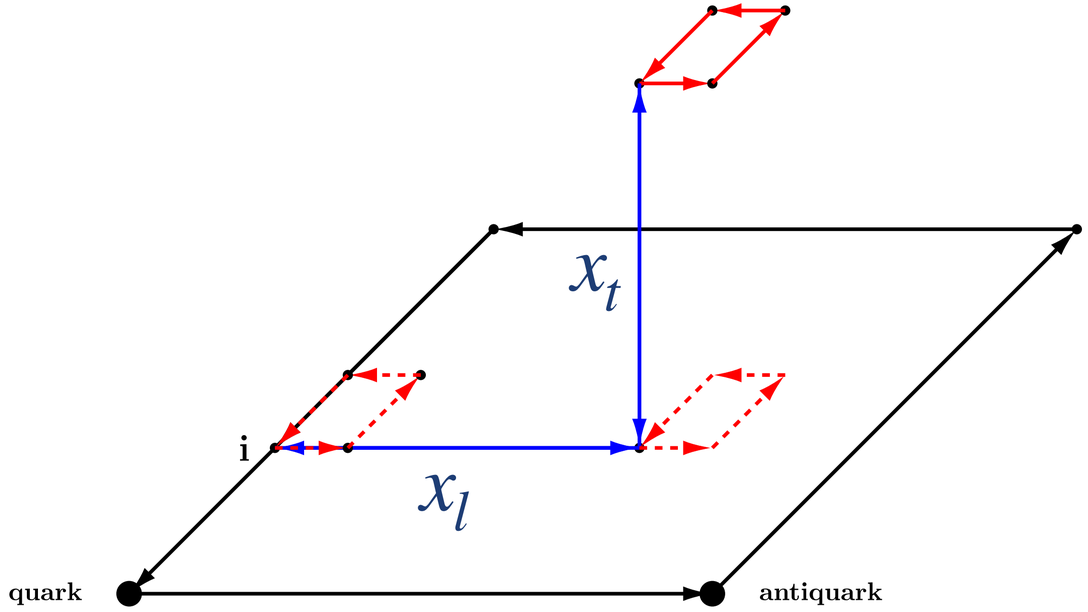

Schwinger line attached to the quark timeline

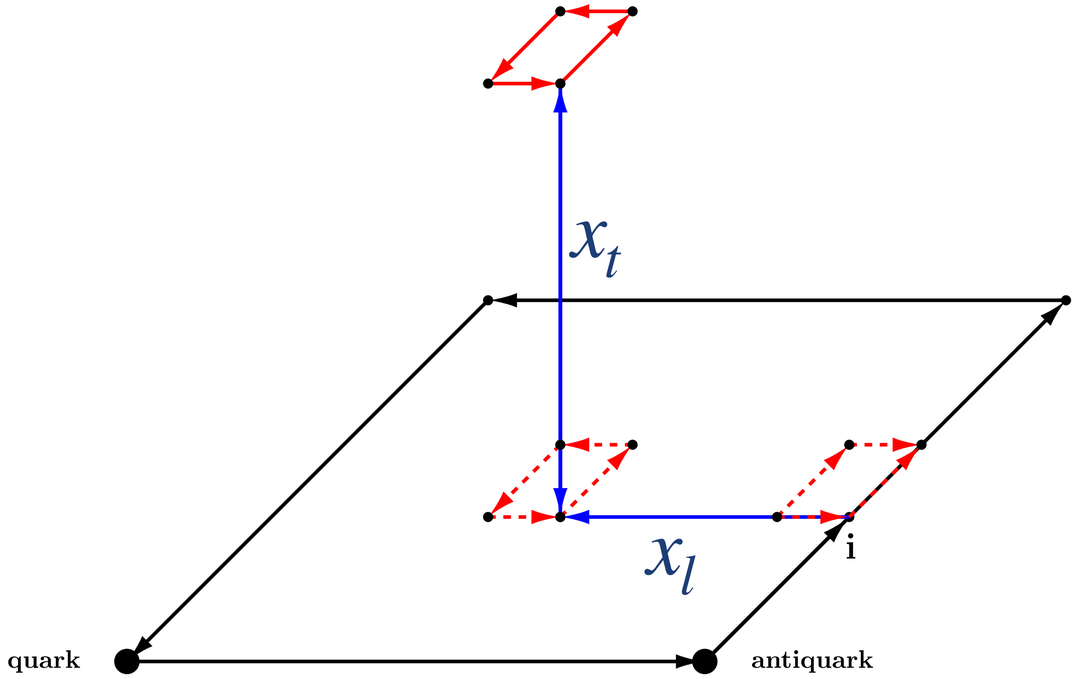

Schwinger line attached to the antiquark timeline

Symmetries of the tensor field components:

$$\mathbf{E}_{\mathbf{x}}^{\mathbf{quark}}(\mathbf{x_l}, \mathbf{x_t}) = \mathbf{E}_{\mathbf{x}}^{\mathbf{antiquark}}(\mathbf{x_l}, \mathbf{x_t}) \qquad \mathbf{E}_{\mathbf{y}}^{\mathbf{quark}}(\mathbf{x_l}, \mathbf{x_t}) = -\mathbf{E}_{\mathbf{y}}^{\mathbf{antiquark}}(\mathbf{x_l}, \mathbf{x_t}) \qquad \mathbf{E}_{\mathbf{z}}^{\mathbf{quark}}(\mathbf{x_l}, \mathbf{x_t}) = -\mathbf{E}_{\mathbf{z}}^{\mathbf{antiquark}}(\mathbf{x_l}, \mathbf{x_t})$$

$48^4 \qquad \beta = 6.880 \qquad T = 43\,\mathrm{MeV}$

Transverse profile of E_x at distance $x_l = 4a = 0.385\,\mathrm{fm}$ from the quark source vs HYP3d smearing steps

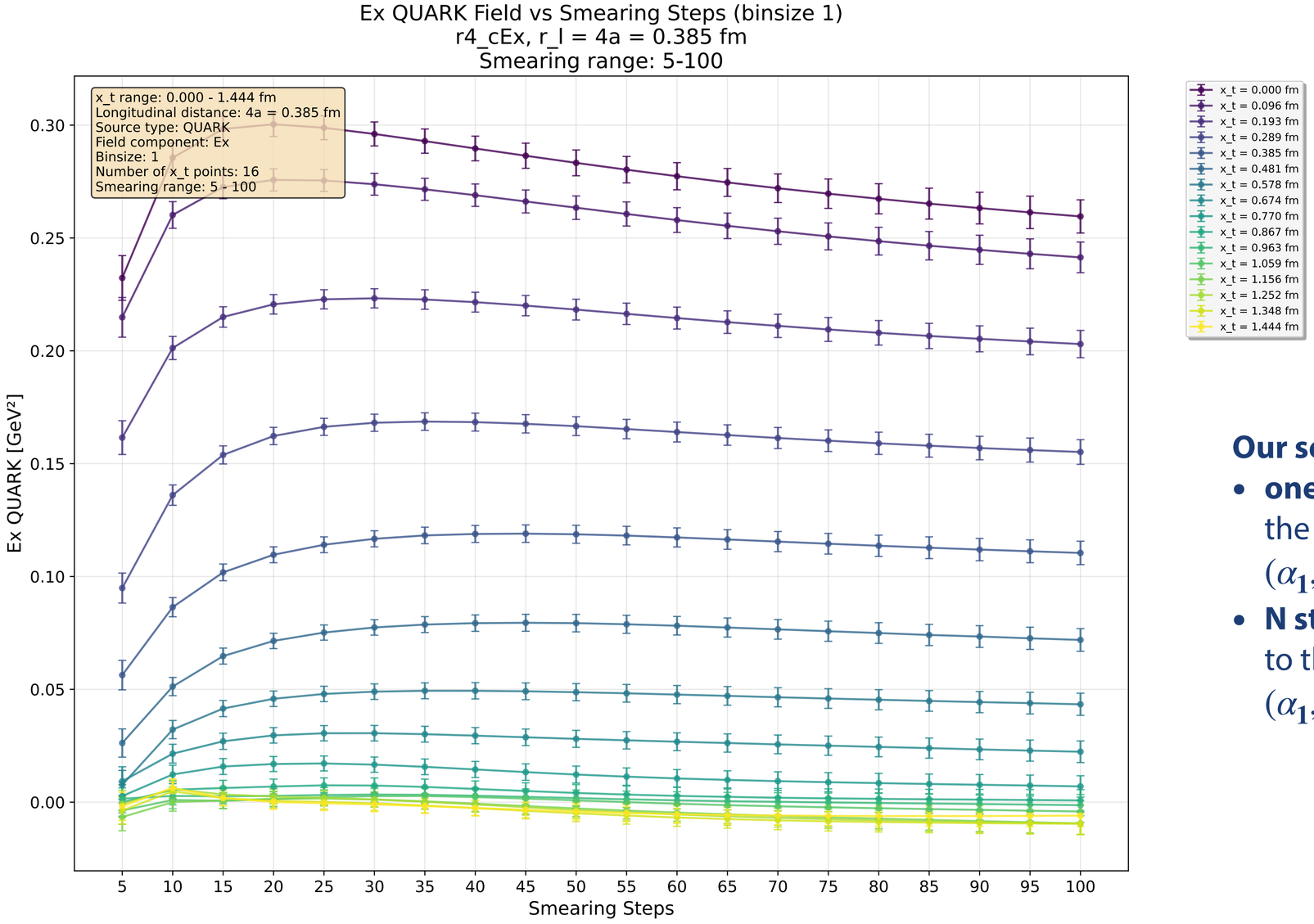

Our setup consists of

- **one step** of 4-dimensional hypercubic smearing on the temporal links (**HYPt**), with smearing parameters $(\alpha_1, \alpha_2, \alpha_3) = (1.0, 1.0, 0.5)$
- **N steps** of hypercubic smearing (**HYP3d**) restricted to the three spatial directions with $(\alpha_1, \alpha_3) = (0.75, 0.3)$.

$48^3 \times 12$ $\beta = 6.880$ $T = 171\,\mathrm{MeV}$

Transverse profile of E_x, E_y, E_z at distance $x_l = 4a = 0.385\,\mathrm{fm}$ from the quark source

50 HYP3d smearing

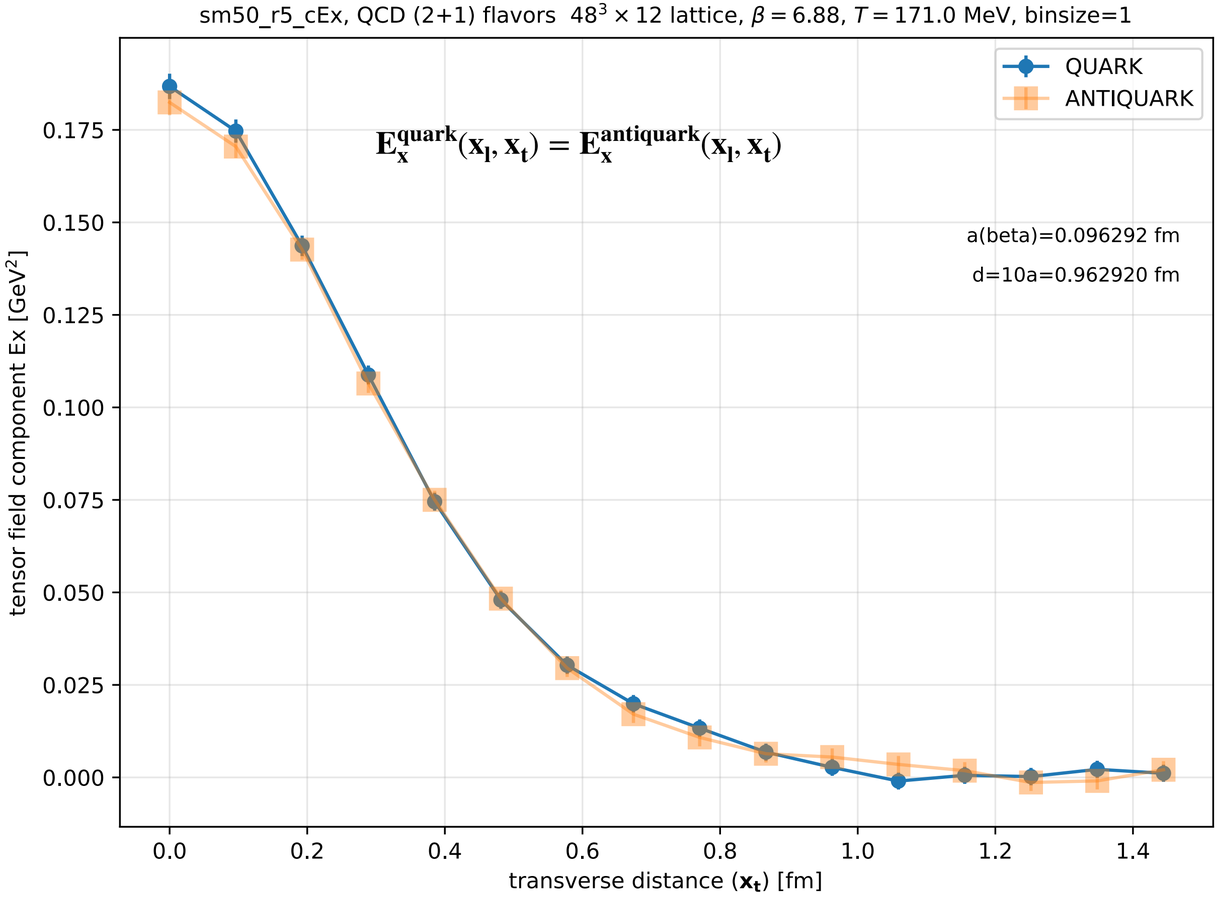

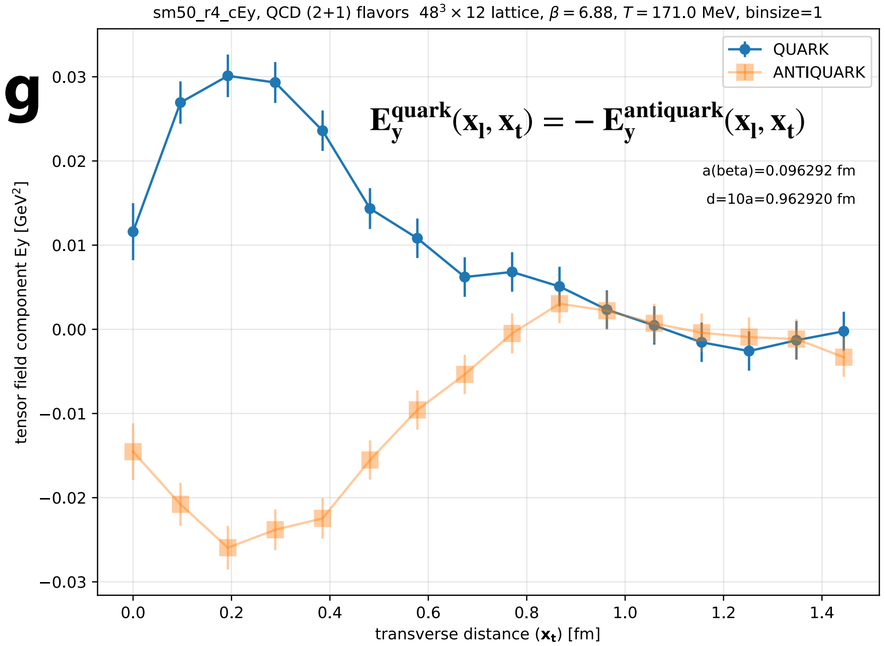

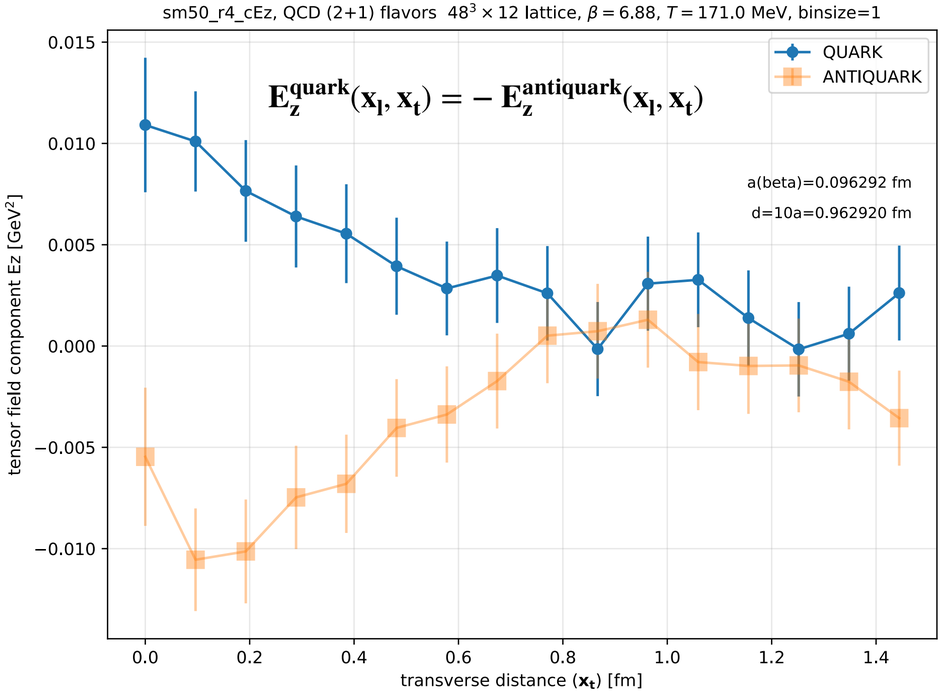

Symmetries of the tensor field components:

$$E_x^{quark}(x_l, x_t) = E_x^{antiquark}(x_l, x_t)$$

$$E_y^{quark}(x_l, x_t) = -E_y^{antiquark}(x_l, x_t)$$

$$E_z^{quark}(x_l, x_t) = -E_z^{antiquark}(x_l, x_t)$$

SCALING CHECK

$T = 205\,\text{MeV} \quad d = 0.963\,\text{fm}$

$\beta = 6.371 \;\; a(\beta) = 0.1605\,\text{fm} \;\; d = 10a = 0.963\,\text{fm}$

$\beta = 6.880 \;\; a(\beta) = 0.0963\,\text{fm} \;\; d = 6a = 0.963\,\text{fm}$

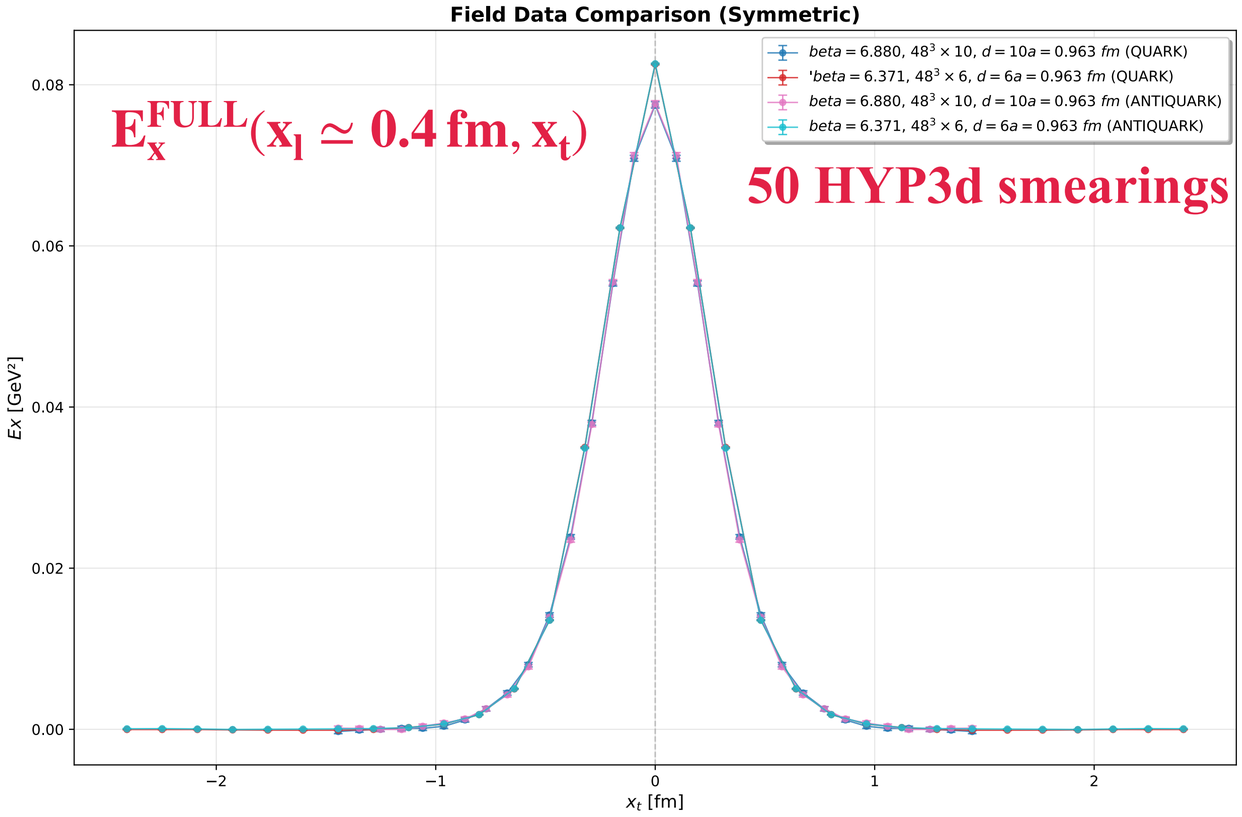

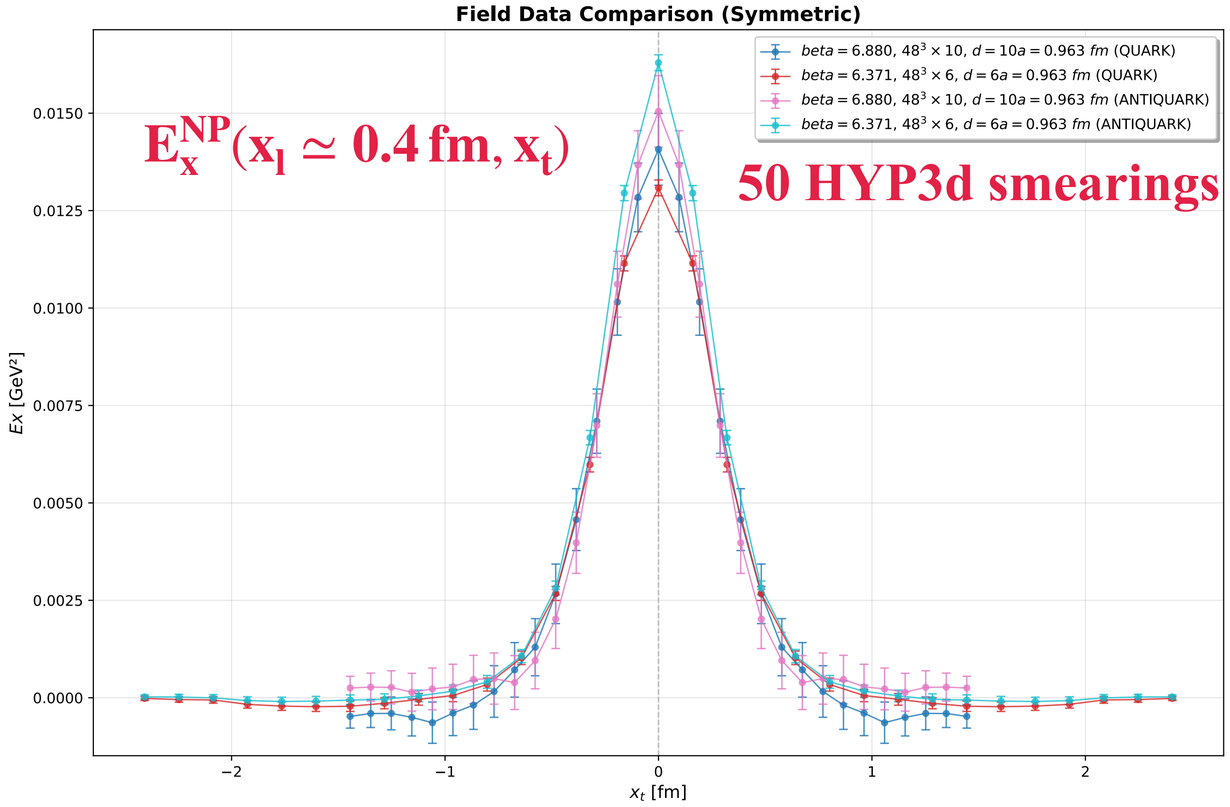

THE FLUX TUBE PROFILE T=43 MeV

QCD (2 + 1) HISQ flavors $m_\pi = 140\,\mathrm{MeV}$

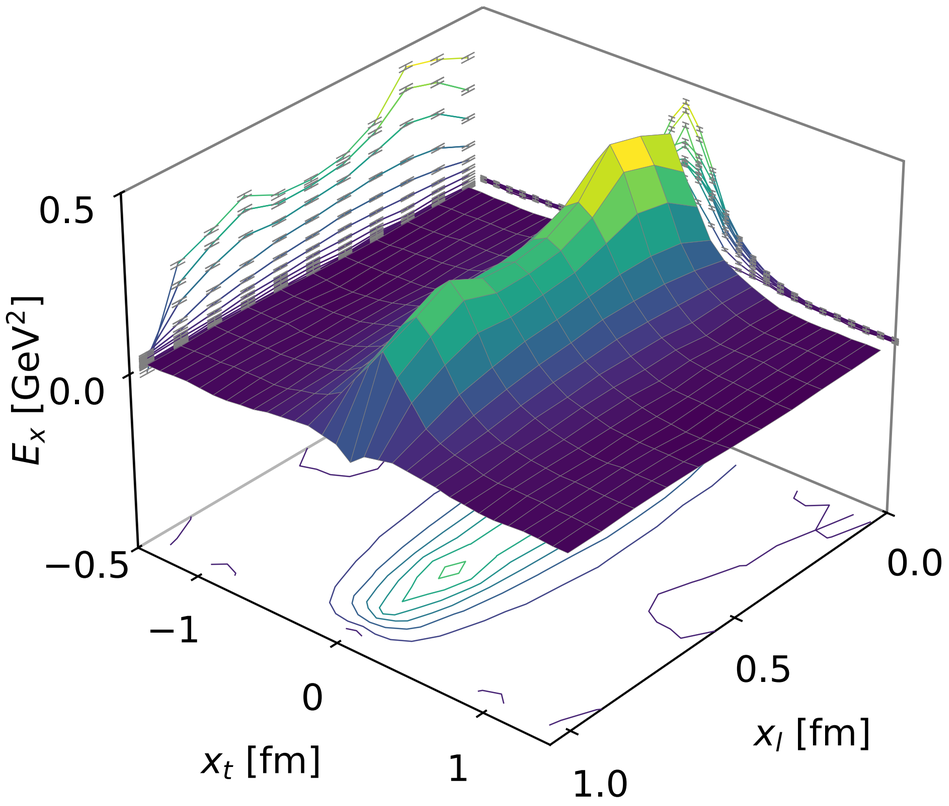

FULL FIELD

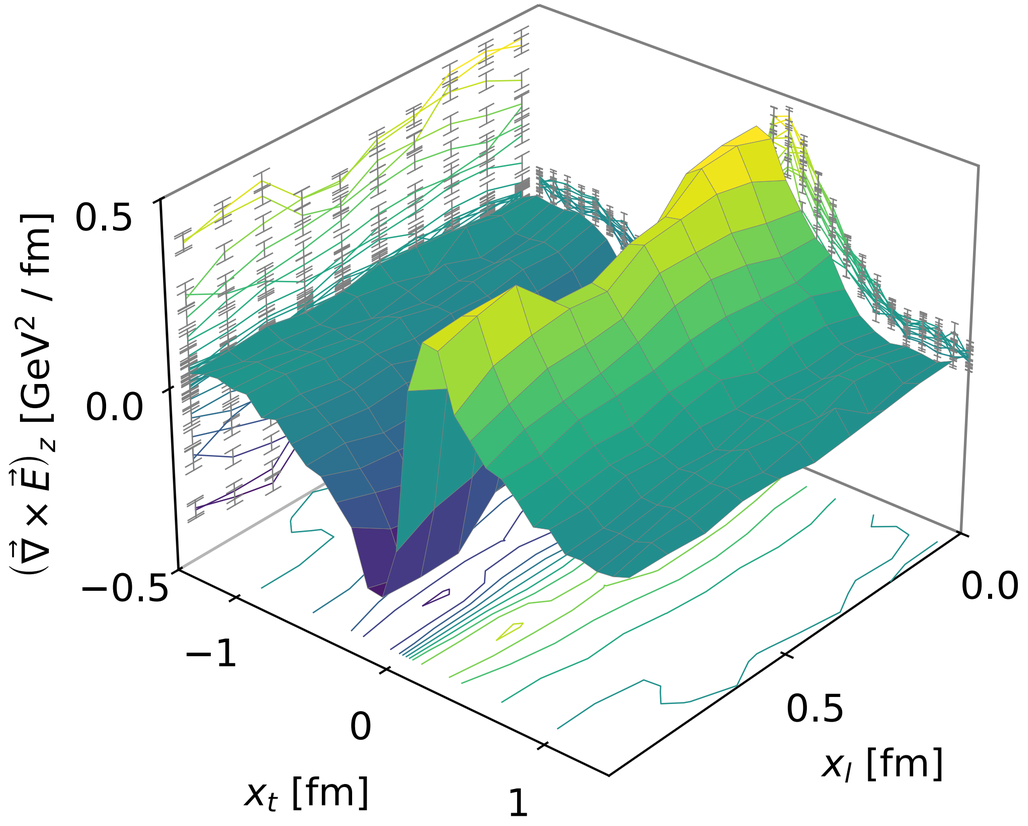

MAGNETIC CURRENT

the presence of a magnetic current density that circulates around the axis of the flux tube that ensures the squeezing of the electric flux tube in the transverse direction according to the Maxwell equation

$$\vec{\nabla} \times \vec{\mathbf{E}}(\vec{\mathbf{x}}) = \vec{\mathbf{J}}_{\mathrm{mag}}(\vec{\mathbf{x}})$$

THE FLUX TUBE PROFILE T=43 MeV

QCD (2 + 1) HISQ flavors $m_\pi = 140\,\mathrm{MeV}$

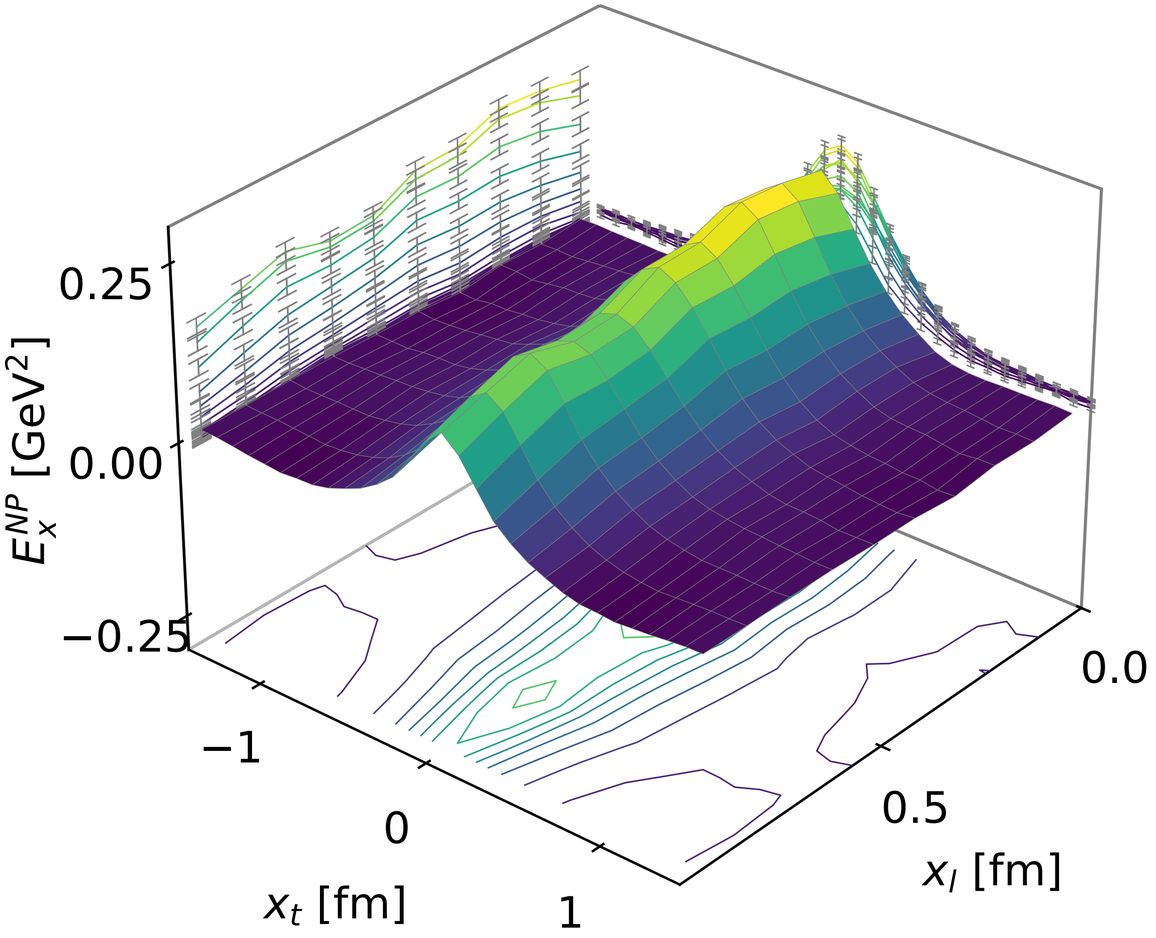

NONPERTURBATIVE FIELD 3d

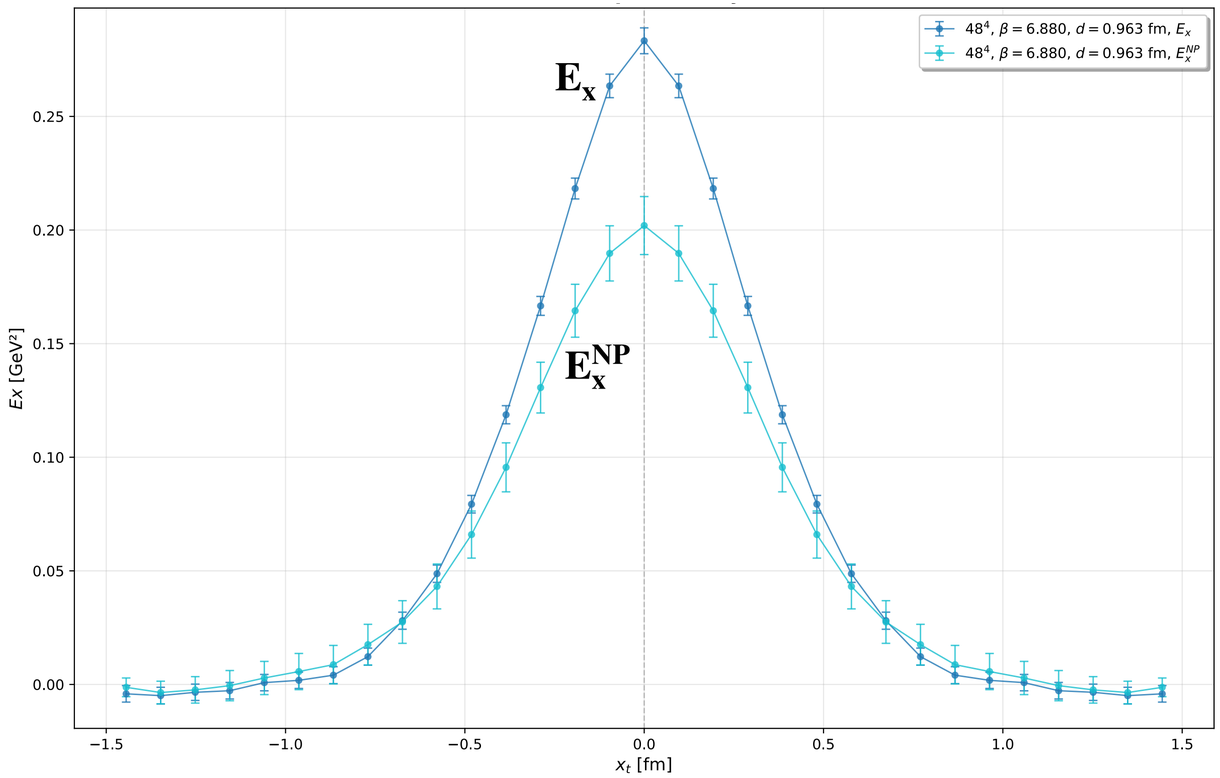

NONPERTURBATIVE FIELD AT MIDPOINT COMPARED TO THE FULL FIELD

THE FLUX TUBE PROFILE VS TEMPERATURE

QCD (2 + 1) HISQ flavors $m_\pi = 140$ MeV

$x_l = 0.433$ fm

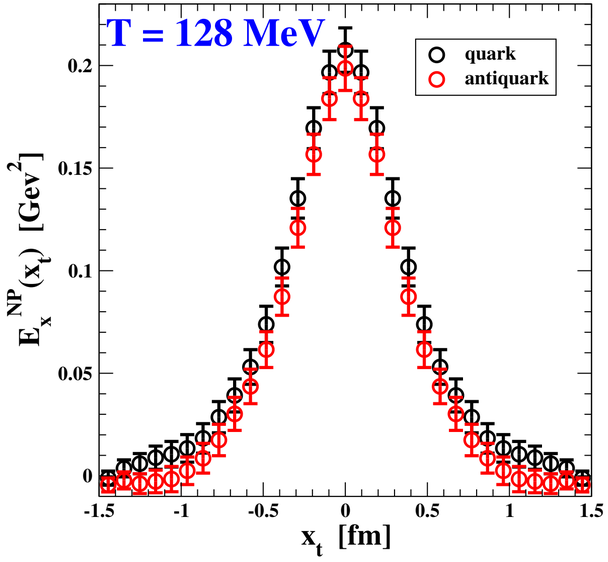

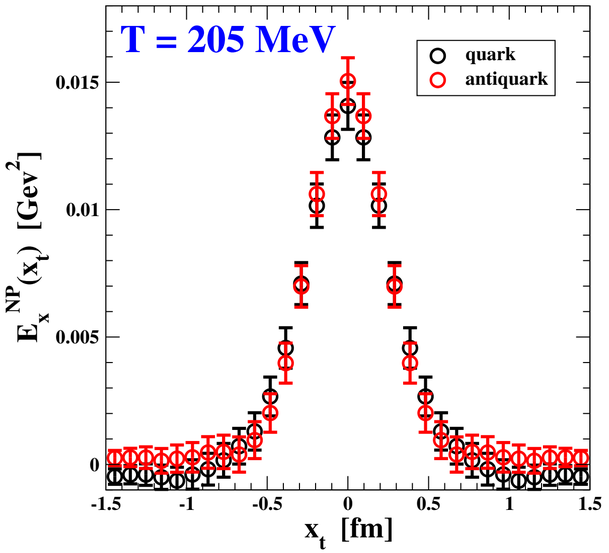

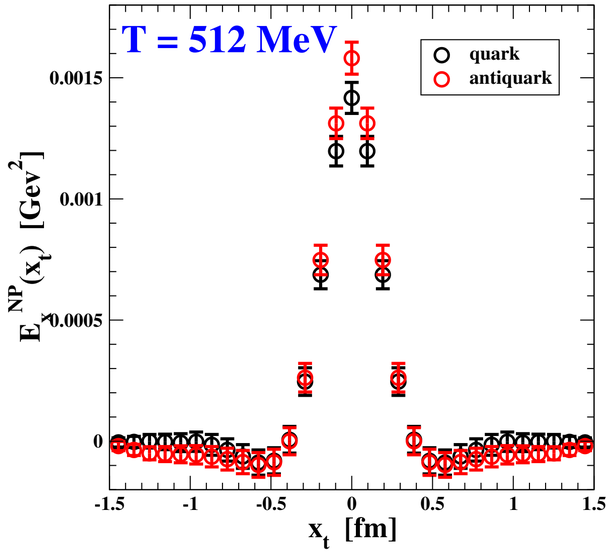

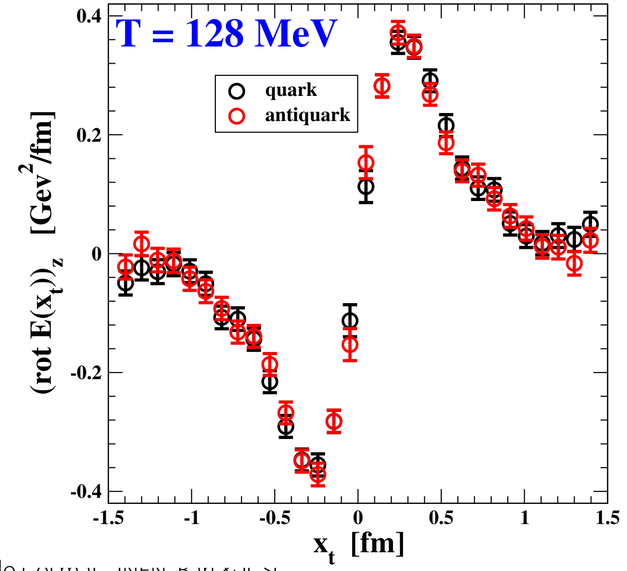

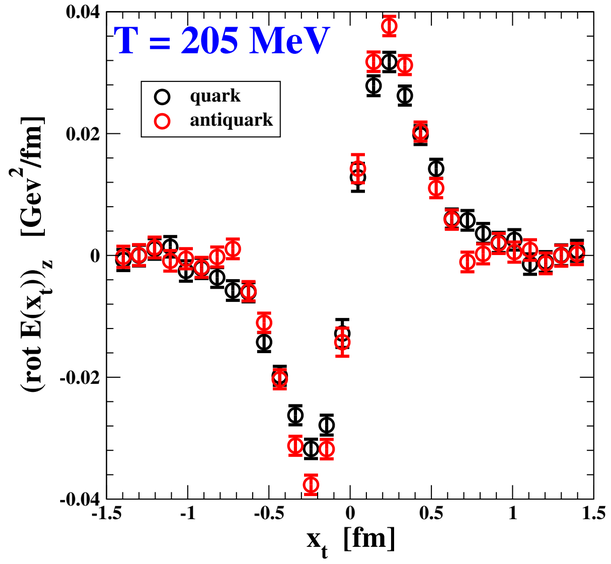

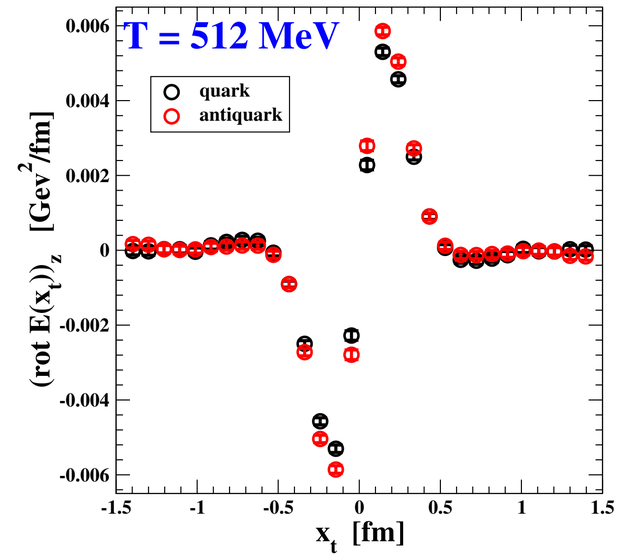

Even at the highest temperature, clear evidence of a non perturbative longitudinal electric field is observed, which remains nearly uniform along the flux-tube structure.

Well beyond the pseudocritical temperature T_c, we are still seeing evidence of color confinement.

$\beta = 6.880,\ 48^3 \times 48,\ \mathrm{T} = 43\,\mathrm{MeV},\ \mathrm{d} = 10\mathrm{a} = 0.963\,\mathrm{fm}$

QUARK CORRELATOR

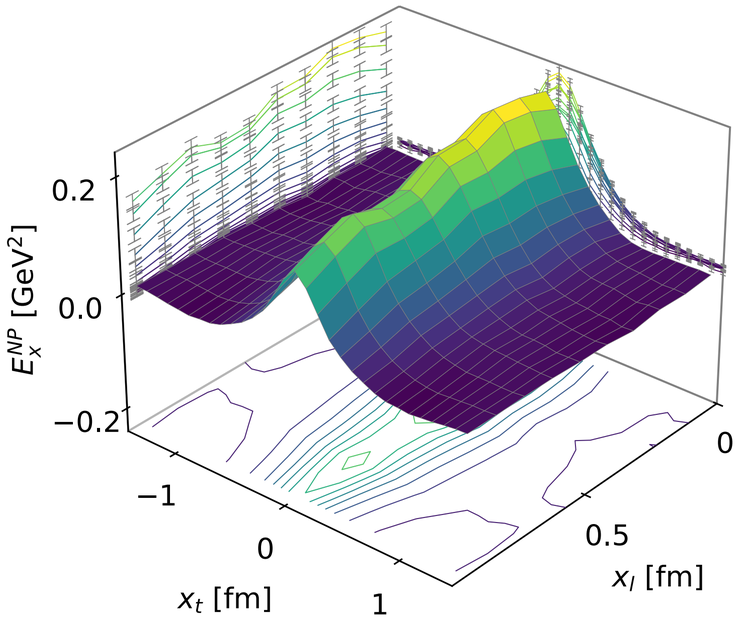

ANTIQUARK CORRELATOR

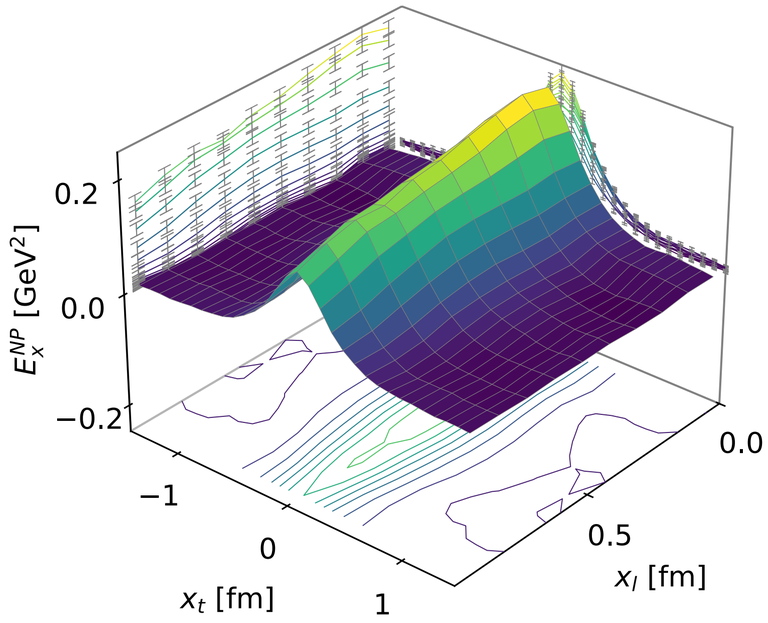

QUARK+ANTIQUARK

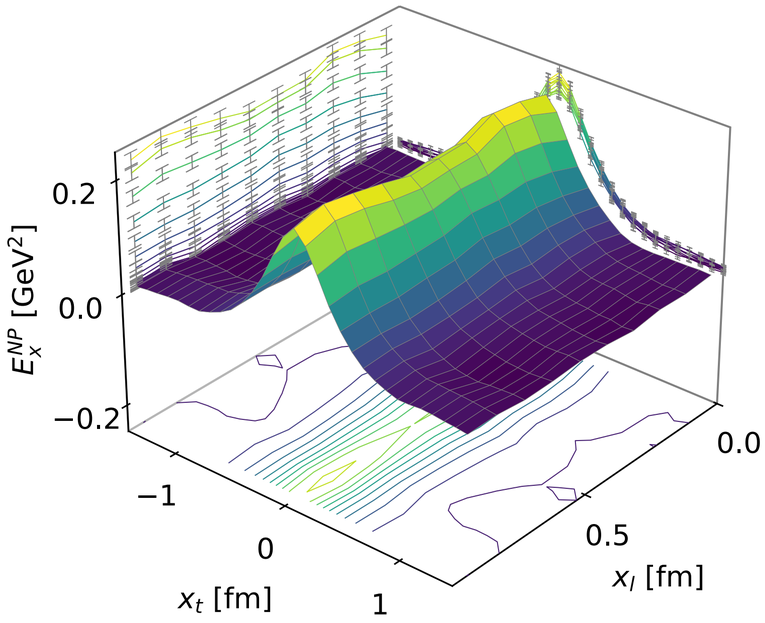

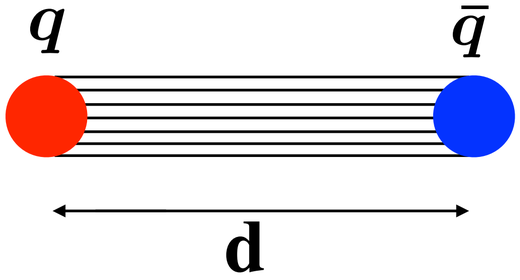

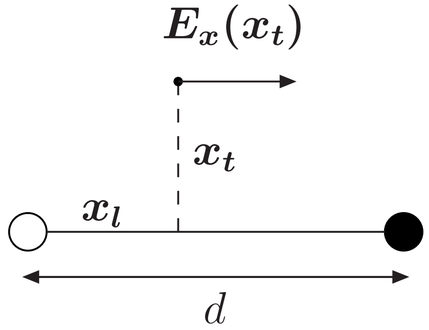

Symmetrization of the nonperturbative field

$$E_x^{NP}(x_l, x_t) = \begin{cases} E_x^{NP,quark}(x_l, x_t) & \text{if } x_l < d/2, \\ E_x^{NP,antiquark}(d - x_l, x_t) & \text{if } x_l \geq d/2. \end{cases}$$

$\beta = 6.880,\ 48^3 \times L_t,\ d = 10a = 0.963\ fm$

T = 43 MeV

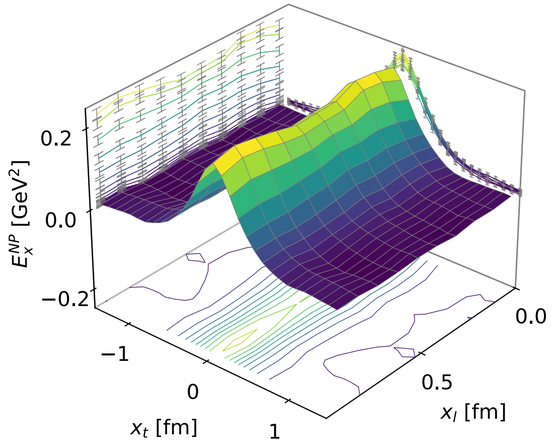

T = 128 MeV

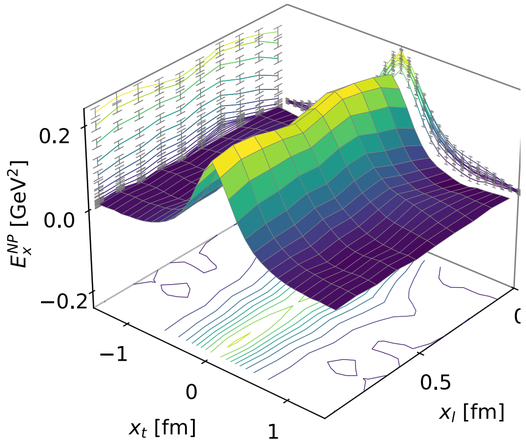

T = 146 MeV

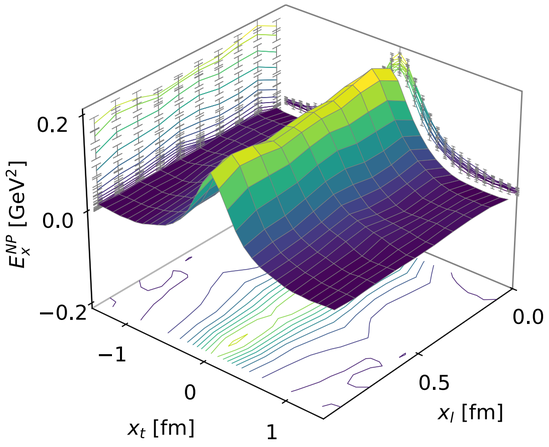

T = 171 MeV

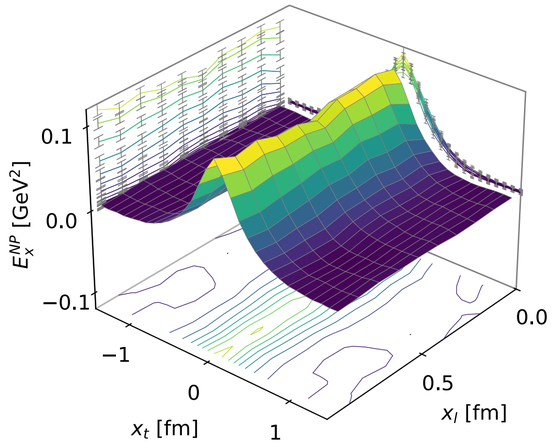

T = 205 MeV

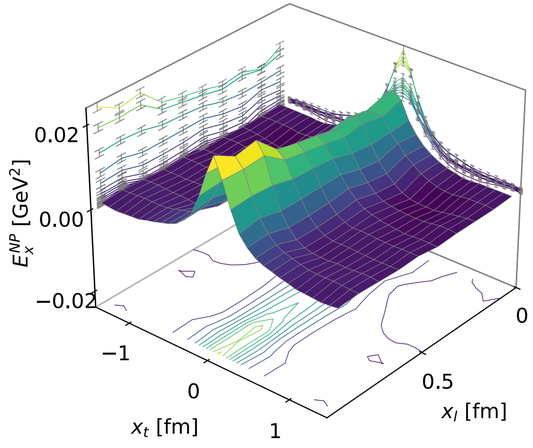

T = 256 MeV

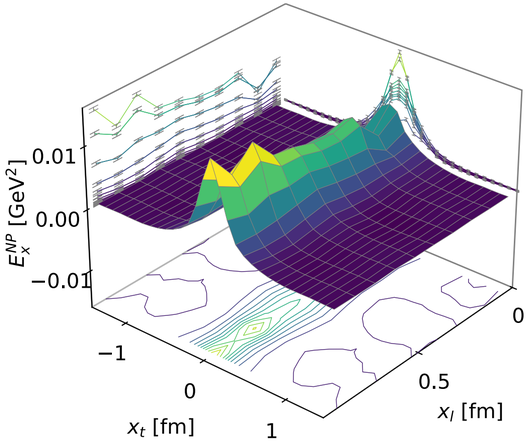

T = 342 MeV

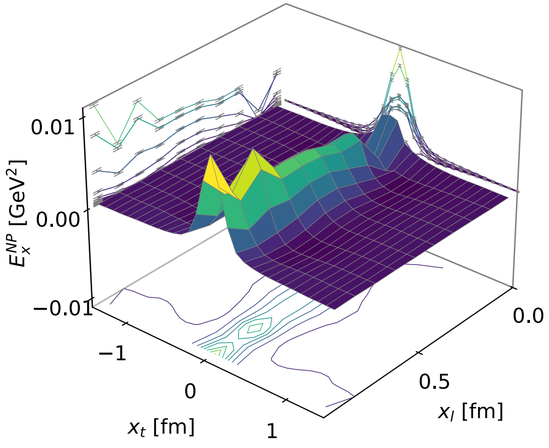

T = 512 MeV

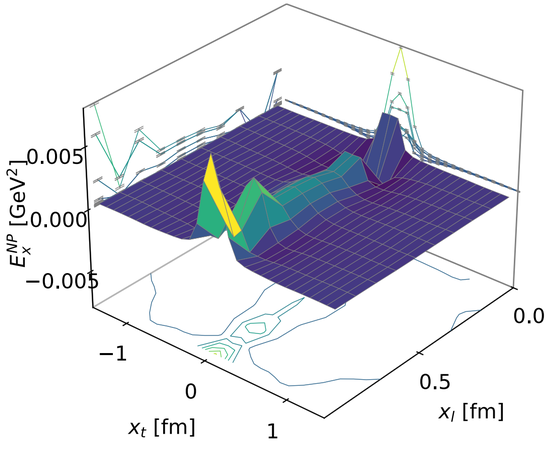

EFFECTIVE STRING TENSION AND WIDTH

ENERGY STORED PER UNIT LENGTH:
ASSUMING CYLINDRICAL SYMMETRY AND CONSTANT FIELD ALONG THE FLUX TUBE, WE INTEGRATE OVER THE TRANSVERSE SECTION

$\beta = 6.880,\ 48^3 \times 48,\ \mathrm{T} = 43\,\mathrm{MeV},\ \mathrm{d} = 10\mathrm{a} = 0.963\,\mathrm{fm}$

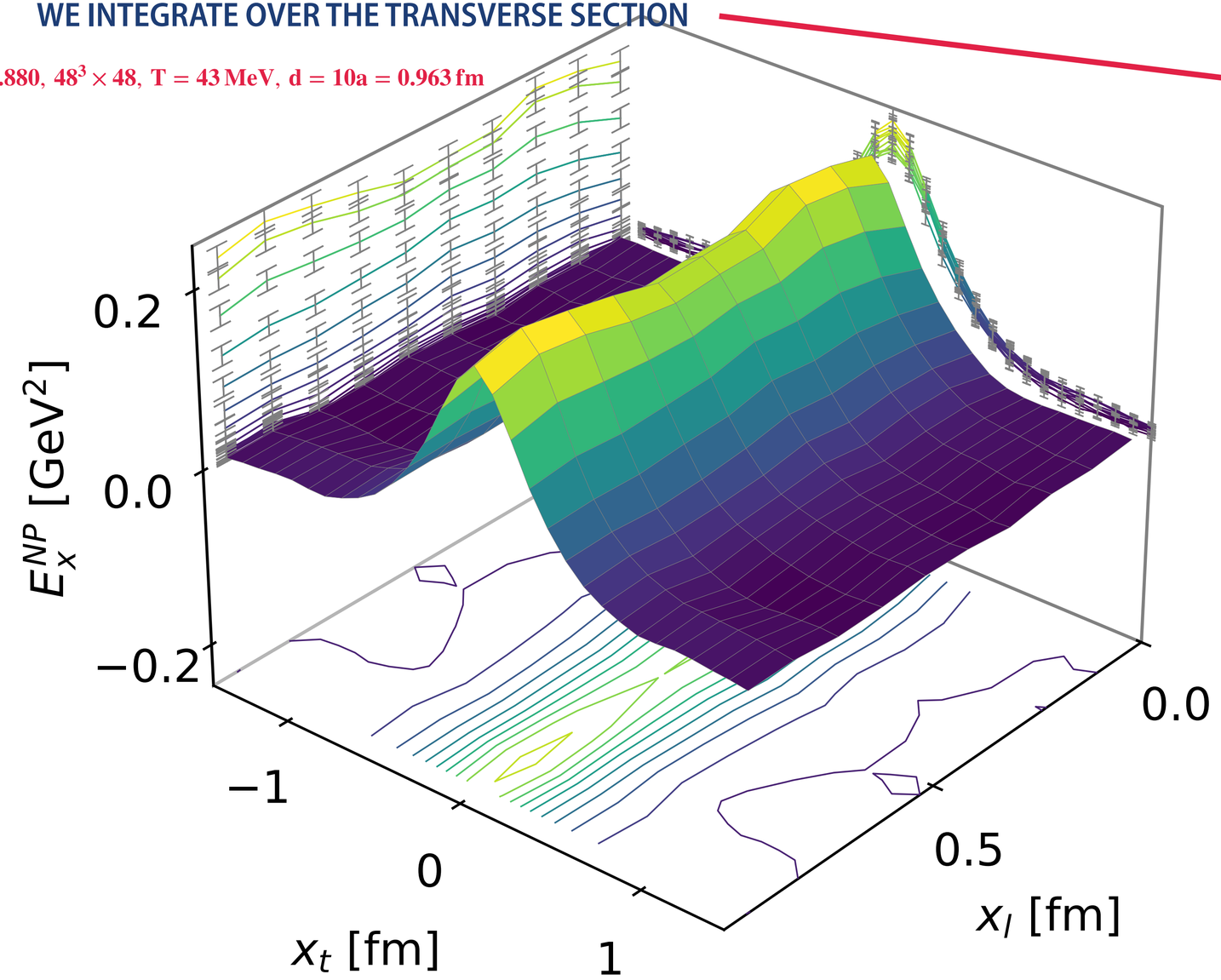

String tension

$$\sigma_{\mathrm{eff}} = \int \mathrm{d}^2\mathrm{x_t}\, \frac{(\mathrm{E_x^{NP}(d/2, x_t)})^2}{2}$$

$$= \pi \int \mathrm{dx_t}\ \mathrm{x_t}\, (\mathrm{E_x^{NP}(d/2, x_t)})^2$$

Width

$$\mathrm{w}^2 = \frac{\int \mathrm{d}^2\mathrm{x_t}\, \mathrm{x_t^2}\, \mathrm{E_x^{NP}(d/2, x_t)}}{\int \mathrm{d}^2\mathrm{x_t}\, \mathrm{E_x^{NP}(d/2, x_t))}}$$

$$= \frac{\int \mathrm{dx_t}\ \mathrm{x_t^3}\, \mathrm{E_x^{NP}(d/2, x_t)}}{\int \mathrm{dx_t}\ \mathrm{x_t}\, \mathrm{E_x^{NP}(d/2, x_t)}}$$

NUMERICAL RESULTS $43\,\mathrm{MeV} \leq T \leq 512\,\mathrm{MeV}$

(from quark correlation function)

lattice	$\beta = 10/g^2$	$a(\beta)$ [fm]	T [MeV]	d [lattice units]	d [fm]	$\sqrt{\sigma_{\mathrm{eff}}}$ [GeV]	w[fm]
$48^3 \times 48$	6.880	0.0963	43	10	0.963	0.405278 (11663)	0.489 221(40185)
$48^3 \times 16$	6.880	0.0963	128	10	0.963	0.442278 (10283)	0.633 737(52862)
$48^3 \times 14$	6.880	0.0963	146	10	0.963	0.363226 (11641)	0.618 508(78860)
$48^3 \times 12$	6.880	0.0963	171	6	0.578	0.323046 (1097)	0.531 699(10469)
$48^3 \times 12$	6.880	0.0963	171	8	0.770	0.255999 (3135)	0.600 661(31716)
$48^3 \times 12$	6.880	0.0963	171	10	0.963	0.178413 (5831)	0.562 810(86458)
$48^3 \times 12$	6.880	0.0963	171	12	1.156	0.092669 (9268)	0.440 789(122465)
$48^3 \times 12$	6.880	0.0963	171	14	1.348	0.080565 (15637)	0.812 643(385497)
$48^3 \times 10$	6.880	0.0963	205	10	0.963	0.022142 (791)	0.368 130(38442)
$48^3 \times 8$	6.880	0.0963	256	10	0.963	0.011389 (218)	0.290 985(12630)
$48^3 \times 6$	6.880	0.0963	342	10	0.963	0.006277 (93)	0.254 471(4238)
$48^3 \times 4$	6.880	0.0963	512	10	0.963	0.001388 (45)	0.160 123(13039)

(from antiquark correlation function)

lattice	$\beta = 10/g^2$	$a(\beta)$ [fm]	T [MeV]	d [lattice units]	d [fm]	$\sqrt{\sigma_{\mathrm{eff}}}$ [GeV]	w[fm]
$48^3 \times 48$	6.880	0.0963	43	10	0.963	0.373637 (11734)	0.494 799(55311)
$48^3 \times 16$	6.880	0.0963	128	10	0.963	0.384049 (9859)	0.475 882(28127)
$48^3 \times 14$	6.880	0.0963	146	10	0.963	0.373842 (11993)	0.649 380(68701)
$48^3 \times 12$	6.880	0.0963	171	6	0.578	0.313870 (1092)	0.476 235(11554)
$48^3 \times 12$	6.880	0.0963	171	8	0.770	0.252945 (3043)	0.570 348(33758)
$48^3 \times 12$	6.880	0.0963	171	10	0.963	0.184021 (5691)	0.535 994(87192)
$48^3 \times 12$	6.880	0.0963	171	12	1.156	0.072523 (8496)	0.282 525(28041)
$48^3 \times 12$	6.880	0.0963	171	14	1.348	0.042945 (25633)	0.334 310(110112)
$48^3 \times 10$	6.880	0.0963	205	10	0.963	0.022166 (760)	0.590 726(124600)
$48^3 \times 8$	6.880	0.0963	256	10	0.963	0.013651 (230)	0.447 764(65751)
$48^3 \times 6$	6.880	0.0963	342	10	0.963	0.006277 (93)	0.249 753(4248)
$48^3 \times 4$	6.880	0.0963	512	10	0.963	0.001514 (46)	0.156 610(12183)

The effective string tension vs T at fixed distance ~1 fm

Thermal behavior of σ_{eff}

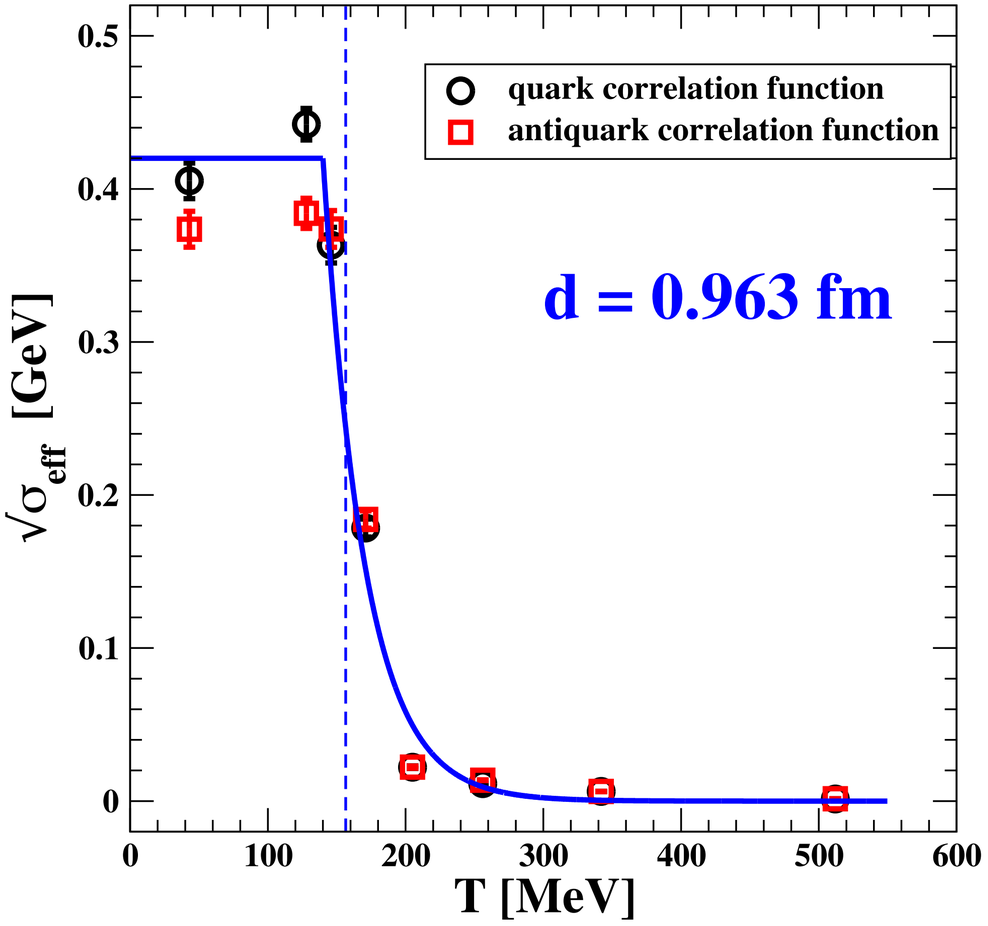

$$T \lesssim 140 - 150 \text{ MeV}$$

The effective string tension stays almost constant to the zero-temperature value albeit with some scatter in the data.
In this low temperature regime the thermal fluctuations do not modify substantially the structure of the flux-tube nonperturbative electric field and the dynamics is governed by wild quantum fluctuations.

$$T \gtrsim T_c = 156.5 \text{ MeV}$$

The quantum dynamics of the hadronic system is clearly dominated by smoother thermal fluctuations such that the values of the effective string tension extracted from the two different connected correlation functions (i.e. quark and antiquark) are in satisfying agreement.

The effective string tension manifests a drastic reduction followed by a more smoother decrease for $T \gtrsim 200$ MeV, suggestive for an exponential decrement with the temperature.

$$\sqrt{\sigma_{eff}}(d,T) = \sqrt{\sigma_{eff}}(0)\ \exp[-\frac{1}{2}\,\mu_{st}(T)\,d]$$

$$\mu_{st}(T) \simeq \begin{cases} 0 & T \lesssim T_0 \\ a_{st}(T - T_0) & T_0 \lesssim T \end{cases}$$

$$T_0 \simeq m_\pi \simeq 140 \text{ MeV} \qquad \sqrt{\sigma_{eff}}(0) \simeq 0.42 \text{ GeV}\ ,\ a_{st} = 13.5(1)$$

a_{st} measures the ratio of the screening mass μ_{st} over the temperature for $T \gg T_0$

The effective string tension vs distance at fixed T=171 MeV

σ_{eff} vs distance at fixed T

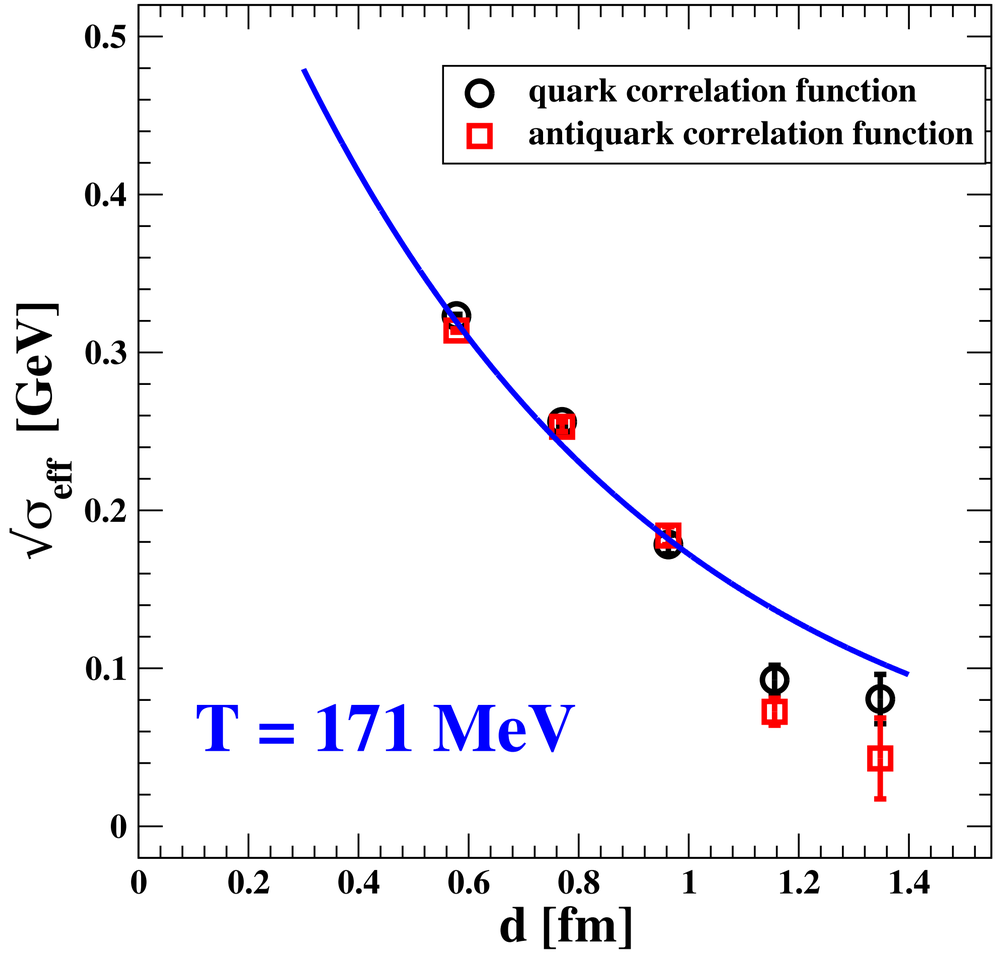

$$\sqrt{\sigma_{eff}}(d, T_1) \;=\; \alpha_{st}\;\exp[-\frac{1}{2}\,\mu_{st}(T_1)\,d]$$

$$\alpha_{st} \;=\; 0.743(28)\ \text{GeV}\ ,\ a_{st} \;=\; 18.6(8)$$

The width of the flux tube vs T at fixed distance ~1 fm

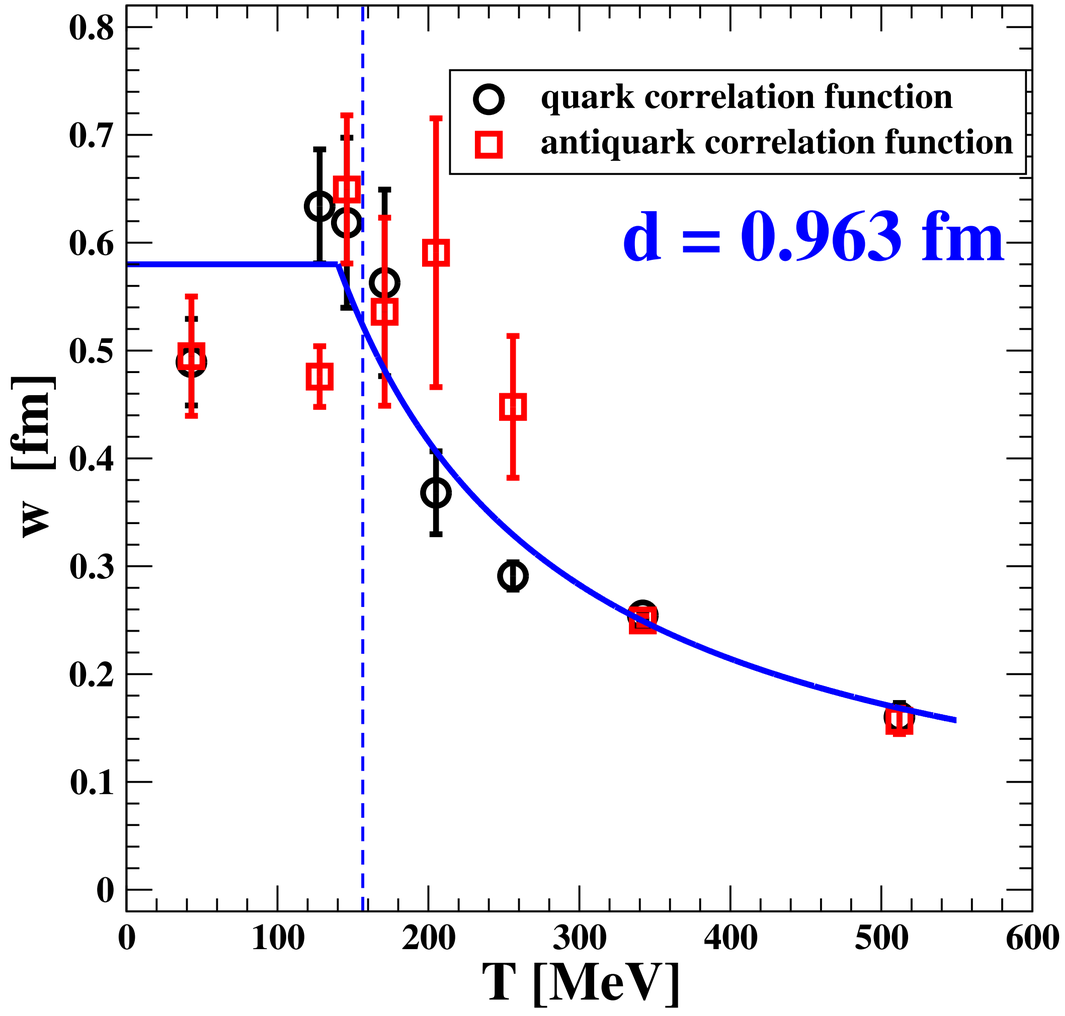

$$\mu_{st}(T) \simeq \begin{cases} w_0 & T \lesssim T_0 \\ \dfrac{w_0}{1 + a_w(T - T_0)} & T_0 \lesssim T \end{cases}$$

$w_0 \simeq 0.58\,\text{fm}$ $\qquad a_w = 0.00657(25)\,\text{MeV}^{-1}$

QUESTIONS TO "ANALYTICAL" COMMUNITY

- Can you explain the relation between the chiral transition and the deconfinement transition? If such a relation exists, which one drives the other?

- In your favourite model of QCD confinement, what are the relevant observables that the lattice people can measure?

SUMMARY

- We have studied the **chromoelectromagnetic field tensor** generated by a quark-antiquark static pair.

- The **longitudinal chromoelectric field forms a flux tube** and it can be characterized by two quantities: σ_{eff} (related to the **string tension**), and the **width** w.

- **SU(3) pure gauge** $\mathrm{T} = 0$ flux tube structure even for relatively large separations ($d > 1.3\,\mathrm{fm}$) of the static quark-antiquark pair.

- **SU(3) pure gauge** $\mathrm{T} \neq 0$ the flux tube structure begins to dissipate above the deconfinement temperature, but a flux tube structure remains even for $\mathrm{T} > 2\mathrm{T_c}$.

- **QCD with (2+1) HISQ flavors at** $m_\pi = 160\,\mathrm{MeV}$, $\mathrm{T} = 0$**:** numerical arguments in favour of a **string breaking distance —>** $1.064\ \mathrm{fm} \lesssim \mathrm{d}^* \lesssim 1.140\ \mathrm{fm}$

- **QCD with (2+1) HISQ flavors at** $m_\pi = 140\,\mathrm{MeV}$, $\mathrm{T} \gtrsim 0$ **(up to** $\mathrm{T} = 512\,\mathrm{MeV} \simeq 3.3\,\mathrm{T_c}$**):**
  - flux tubes still at $\mathrm{T} \simeq 3.3\,\mathrm{T_c}$;
  - Effective string tension drops fast with increasing T and/or **distance** between quark and antiquark sources.

TODO:

- **Study of string breaking with QCD (2+1) HISQ flavors on the line of constant physics with** $m_\pi = 140\,\mathrm{MeV}$.

THANK YOU FOR YOUR ATTENTION !